Breast Cancer (2010) 17:118–124
DOI 10.1007/s12282-009-0113-0

ORIGINAL ARTICLE

Clinicopathological analyses of triple negative breast cancer using surveillance data from the Registration Committee of the Japanese Breast Cancer Society

Hirotaka Iwase · Junichi Kurebayashi · Hitoshi Tsuda · Tomohiko Ohta · Masafumi Kurosumi · Kazuaki Miyamoto · Yutaka Yamamoto · Takuji Iwase

Received: 15 January 2009 / Accepted: 10 March 2009 / Published online: 23 May 2009

Abstract
Background Triple negative (TN) breast cancer is defined as a subtype that is negative for estrogen receptor (ER), progesterone receptor (PgR), and human epidermal growth factor receptor 2 (HER2). To clarify the characteristics of TN breast cancer, surveillance data of the Registration Committee of the Japanese Breast Cancer Society were analyzed.
Method Of 14,748 cases registered in 2004, 11,705 (79.4%) were examined for ER, PgR, and HER2. Of these, the most prevalent (53.8%) was a hormone-responsive subtype with ER positive/PgR positive/HER2 negative, followed by TN subtype (15.5%).
Results The proportion of postmenopausal patients was relatively high in the TN subtype. This cancer was diagnosed at a slightly advanced stage and with more cases positive for lymph node metastases than other subtypes. Morphologically, the TN subtype was more frequently classified as solid-tubular carcinoma. Mucinous, tubular, or secretary carcinomas were frequently found in the hormone receptor positive/HER2 negative subtype, while squamous cell carcinoma, spindle cell carcinoma, and metaplastic

H. Iwase · J. Kurebayashi · H. Tsuda · T. Ohta · M. Kurosumi · K. Miyamoto
Member of the Research Group,
Japanese Breast Cancer Society, Tokyo, Japan

H. Iwase (✉) · Y. Yamamoto
Department of Breast and Endocrine Surgery,
Kumamoto University, 1-1-1 Honjo,
Kumamoto 860-8556, Japan
e-mail: hiwase@kumamoto-u.ac.jp

Y. Yamamoto
e-mail: ys-yama@triton.ocn.ne.jp

J. Kurebayashi
Department of Breast and Thyroid Surgery,
Kawasaki Medical University, Okayama, Japan
e-mail: kure@med.kawasaki-m.ac.jp

H. Tsuda
Pathology Section, Clinical Laboratory Division,
National Cancer Center Hospital, Tokyo, Japan
e-mail: hstsuda@ncc.go.jp

T. Ohta
Division of Breast and Endocrine Surgery,
Department of Surgery, St. Marianna University School of Medicine, Kawasaki, Japan
e-mail: to@marianna-u.ac.jp

M. Kurosumi
Department of Pathology, Saitama Prefecture Cancer Center,
Saitama, Japan
e-mail: mkurosumi@cancer-c.pref.saitama.jp

K. Miyamoto
Department of Surgery, National Hospital Organization Kure Medical Center/Chugoku Cancer Center, Kure, Japan
e-mail: miyamotok@kure-nh.go.jp

T. Iwase
Director of the Registration Committee of the Japanese Breast Cancer Society, Tokyo, Japan

T. Iwase
Department of Breast Clinic, Cancer Institute Ariake Hospital,
Tokyo, Japan
e-mail: takiwase@nifty.com

carcinoma with bone/cartilage metaplasia were very frequently found in the TN group. Apocrine carcinoma was also found very frequently in the TN group. Selection of chemotherapy was not based on receptor subtypes, but was determined by the degree of tumor progression.

Conclusions Although TN types are similar to basal-like breast tumor, as determined by gene profiling, their diagnosis needs verification by determination of the level of epidermal growth factor receptor or cytokeratin 5/6 expression. TN type should be examined further for immunohistochemical features and analyzed for prognostic details in this cohort.

Keywords Triple negative tumor · Breast cancer · Surveillance data

Introduction

Triple negative (TN) breast cancer represents a subtype that is negative for the three main prognostic/predictive receptors for breast cancer, namely, estrogen receptor (ER), progesterone receptor (PgR), and HER2 (human epidermal growth factor receptor type 2) [1]. ER and/or PgR positive cancer, which means hormone receptor (HR)-positive cancer, usually responds to endocrine therapy. Cancers scored immunohistochemically as 3+ or 2+ and that are 'fluorescence in situ hybridization' (FISH)-positive are regarded as HER2-positive and are targets for treatment with trastuzumab and other agents aimed at HER2. However, currently no targeted therapeutic agents have been identified specifically for TN breast cancer, and the only option at present is conventional systemic chemotherapy. In this context, it is essential to be familiar with the biological features of TN breast cancer in order to develop the best therapeutic strategy [1–3].

An alternative approach to subtyping breast cancers has been developed by Sørlie et al. [4, 5], who classified breast cancer into four or more intrinsic subtypes on the basis of gene profiling acquired from microarray analyses of a large number of breast cancer tissue specimens. In their classification, the first was called a basal-like subtype; it shared some characteristics with basement membrane cells and had a high proliferative capability [6]. The second was the HER2 (ErbB2) subtype, in which HER2 and related genes were overexpressed and ER-related genes were under expressed. This subtype was also relatively highly proliferative and expected to respond to trastuzumab. The third subtype had normal epithelium (normal-like subtype), but its other significant features have yet to be established. The fourth was called the luminal subtype, which expressed various amounts of ER-related genes that could be further subclassified into luminal A or B. If a connection can be found between the intrinsic subtypes and 'classic' breast cancer subtypes based on receptor status, the correlation is best understood by contrasting the basal-like subtype to TN breast cancer, as the former is positive for cytokeratin 5/6 or epidermal growth factor receptor (EGFR) (HER1).

The basal-like subtype accounts for 15–20% of breast cancers, irrespective of the method of analysis or ethnic group [6]. However, premenopausal African–American patients have a significantly higher incidence of this subtype compared to other patients [7]. It is well known that the pathological and biological characteristics of breast cancer are significantly worse in young African–American patients and that they show a clinically poor prognosis. In contrast, the basal-like subtype is relatively uncommon in breast cancers diagnosed in Japanese women; in 793 breast cancer patients, only 8% were this genetic subtype [8]. A significant overlap has been repeatedly demonstrated between the biological and clinical characteristics of sporadic TN breast cancers and basal-like subtypes, and breast carcinomas arising in BRCA1 mutation carriers [5].

In the receptor subtype determination, there is an ongoing debate on how to determine what to take as the cutoff value for deciding the positive/negative expression levels of hormone receptors. For example, there is no agreement at present on whether 'negative' should be based on: (1) no expression, (2) a score of 0 or 2 on the Allred Score [9], which takes into account the number of positive cells and the intensity of staining for the receptor in question, or (3) the proportion of receptor-positive cells less than 10% [10].

The purpose of this study was to disclose clinicopathological features of TN breast cancer. With the support of the Registration Committee of the Japanese Breast Cancer Society, we analyzed about 11,000 cases registered in 2004 in order to classify them by receptor subtypes based on expression levels of ER/PgR/HER2 and to analyze the clinicopathological characteristics of TN tumors.

Materials and methods

Basic data of patients

Comprehensive data on breast cancer patients diagnosed in Japan in 2004 were registered by the Registration Committee of the Japanese Breast Cancer Society, who reported the final registry data in 2008, although patient outcome data have not been published yet. The registrations were made by 352 institutions and included 14,749 cases. The data collected were: age, clinicopathological features of the tumor including size, presence of lymph node metastases, and receptor status (ER, PgR, and HER2), surgical techniques, and regimens of chemotherapy.

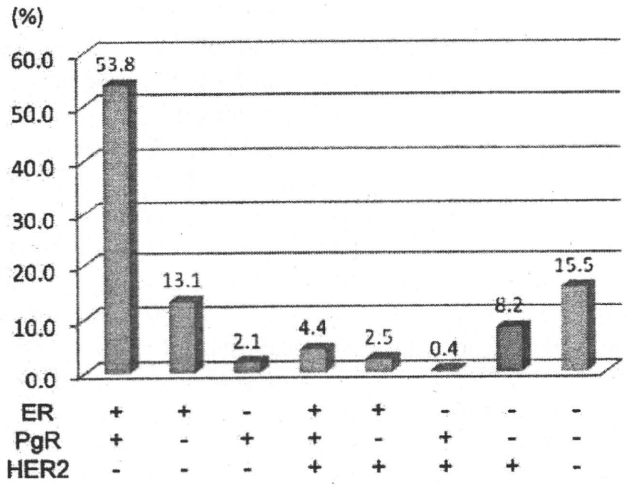

Fig. 1 Breast cancer surveillance data reported by the Japanese Breast Cancer Society

Individual participating institutions determined ER, PgR, and HER2 status by their own in-house method, as well as the other criteria for the registration. In 2004 the status of ER and PgR was being determined by the immunohistochemical (IHC) technique using monoclonal antibodies. Additionally, the cutoff level was mainly adopted to a score of between 2 and 3 on the Allred Score [9], or 10% as a staining proportion [10]. Tumors that were immunohistochemically scored as 3+, or scored 2+ with FISH-positive, were regarded as HER2-positive in a majority of individual participating institutions.

Subanalysis of receptors

Subanalysis was performed by permission of the Registration Committee and the Board of the Japanese Breast Cancer Society. Status of ER, PgR, and Her2 had been determined in 11,705 cases (79.4% of all registered cases), of which 1,819 cases (15.5%) were registered as negative for any one of ER/PgR/HER2. The most prevalent subtype was ER+/PgR+/HER2− (53.8%), followed by TN breast cancer (15.5%) (Fig. 1).

Receptor subtypes were divided according to their ER/PgR/HER2 profiles: the HR+/HER2− subtype was positive for ER and/or PgR and negative for HER2; the HR+/HER2+ subtype was positive for ER and/or PgR and positive for HER2; the HR−/HER2+ subtype was negative for both ER and PgR and positive for HER2; the triple negative (TN) subtype was negative for all three receptors, ER, PgR, and HER2 (Table 1)

Statistical processing

Fischer's exact test was used to compare various prevalence rates among the groups. Unpaired *t* test was employed to make inter-group comparisons in the number of cases and mean values. A significance level was set at less than 0.01 when multiple comparisons were required between four groups.

Table 1 Receptor subtype and status

Subtype	ER/PgR/HER2 status	
	Receptor profile	ER/PgR/HER2
HR+/HER2−	ER+ and/or PgR+, HER2−	+/+/−, +/−/−, −/+/−
HR+/HER2+	ER+ and/or PgR+, HER2+	+/+/+, +/−/+, −/+/+
HR−/HER2+	ER− and PgR−, HER2+	−/−/+
Triple negative	ER−, PgR− and HER2−	−/−/−

+, Positive; −, negative

Results

Patient backgrounds

The relative proportions of the four cancer subtypes were: HR+/HER2− subtype, 68.7%; HR+/HER2+ subtype, 7.6%; HR−/HER2 subtype, 8.3%; and TN subtype, 15.4%. There was no difference in mean age between the groups. The incidence of bilateral breast cancer was significantly lower in HER2-positive subtypes than in HER2-negative subtypes ($P = 0.040$). The proportion of premenopausal patients was significantly greater in HR-positive groups (i.e., HR+/HER2− and HR+/HER2+ subtypes) than in the HR-negative groups (i.e., HR−/HER2+ or TN subtype) ($P < 0.001$). There were no significant differences between subtypes with respect of family history of breast cancer, height, body weight, or body mass index (BMI) (Table 2). Regarding disease stage, 37.2% of the HR+/HER2− subtype were diagnosed at stage I, indicating relatively early initiation of therapy, whereas the prevalence of stage I at diagnosis in HER2 was only 14.2%, which meant these patients received their first treatment at the slightly advanced stages of II–IV (Fig. 2).

Clinical findings

HR+/HER2− subtype was detected at an earlier stage than the other subtypes, that is, when the tumor was somewhat smaller in diameter, and compared advantageously in the incidence of node metastases especially with the ER−/HER2+ subtype. There was a tendency for the incidence of distant metastases to be higher in the HER2-positive groups (i.e., ER+/HER2+ and ER−/HER2+ subtypes) and for breast-conserving therapy to be less frequently performed in patients with the HR−/HER2+ subtype (Table 2).

Table 2 Patient background and clinicopathological data

	Receptor subtype			
	HR+/HER2−	HR+/HER2+	HER2	TN
Number of patients (%)	8,039 (68.7)	892 (7.6)	977 (8.3)	1,797 (15.4)
Age median (range)	56 (NR–100)	54 (23–93)	56 (22–95)	57.5 (NR–94)
Ratio of bilateral breast cancer (%)	6.6[b]	5.9[a]	4.8[a]	6.2[b]
Incidence of breast cancer family history (%)	8.6	8.4	24.1	28.1
Ratio of premenopausal patients (%)	37.1[c]	38.8[c]	24.1[d]	28.1[d]
Height (cm) mean ± SD	154.3 ± 6.3	154.9 ± 6.1	154.0 ± 6.2	153.8 ± 6.3
Weight (kg) mean ± SD	54.7 ± 9.0	54.5 ± 8.8	53.9 ± 8.6	54.2 ± 9.0
BMI mean ± SD	23.0 ± 3.7	22.7 ± 3.5	22.7 ± 3.3	22.9 ± 3.5
Tumor size (cm) mean ± SD	2.6 ± 2.1[e]	3.2 ± 2.2	3.5 ± 2.6[f]	3.4 ± 2.7
Incidence of positive lymph node involvement (%)	20.6	34.9	38.5	32.2
Incidence of distant metastasis (%)	2.5	5.6	5.6	3.2
Incidence of breast-conserving surgery (%)	53.9	41.3	35.1	45.0

NR no record

[a] HER2 positive versus [b]HER2 negative according to ratio of bilateral breast cancer; $P = 0.040$, Fisher's exact probability test

[c] Hormone receptor-positive group versus [d]hormone receptor-negative group according to the ratio of premenopausal patients; $P < 0.0001$, Fisher's exact probability test

[e] HR+/HER2− subtype versus [f]TN subtype according to tumor size; $P < 0.00001$, standard t test of mean and standard deviation (SD)

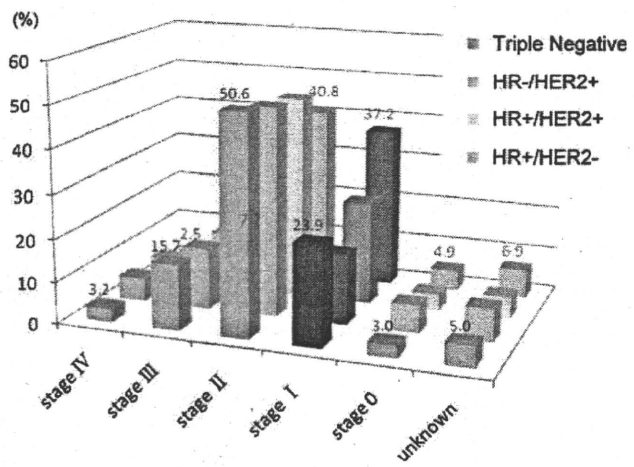

Fig. 2 Stage at diagnosis by receptor subtype

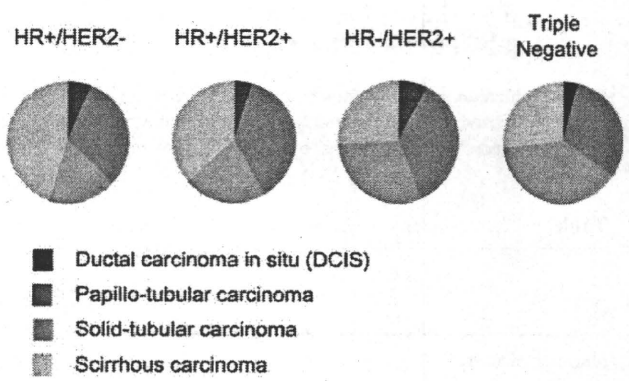

Fig. 3 DCIS and histological subtypes of invasive ductal carcinoma (IDC) by receptor subtype

Pathological findings

From a viewpoint of morphologic classification, whereas scirrhous carcinoma was most frequently found in ER+/HER2− subtype, solid-tubular carcinoma prevailed in TN breast cancer (Fig. 3). As to breast cancers of special types, mucinous carcinoma occurred rarely in the TN group, but was quite frequent among ER+/HER2− subtype patients (Fig. 4a). Invasive lobular carcinoma was found reasonably frequently in the HR+/HER2− type (Fig. 4b). Tubular and secretary carcinomas were mostly found in patients with a HR+/HER2− subtype (Fig. 4c).

Medullary carcinomas were observed frequently in the TN group (Fig. 4d). Squamous cell carcinoma, spindle cell carcinoma, or metaplastic carcinoma with bone/cartilage metaplasia was likewise very common in patients in the TN subtype (Fig. 4e). This group also included the highest percentages of apocrine carcinomas (Fig. 4f).

Selection of chemotherapeutic regimens

Two main chemotherapeutic regimens were administered: (1) anthracycline-containing regimens (ACR), which included: doxorubicin plus cyclophosphamide (AC), epirubicin plus C (EC), C plus A plus 5-fluorouracil (CAF) and CEF, and (2) taxane (paclitaxel or docetaxel)-containing

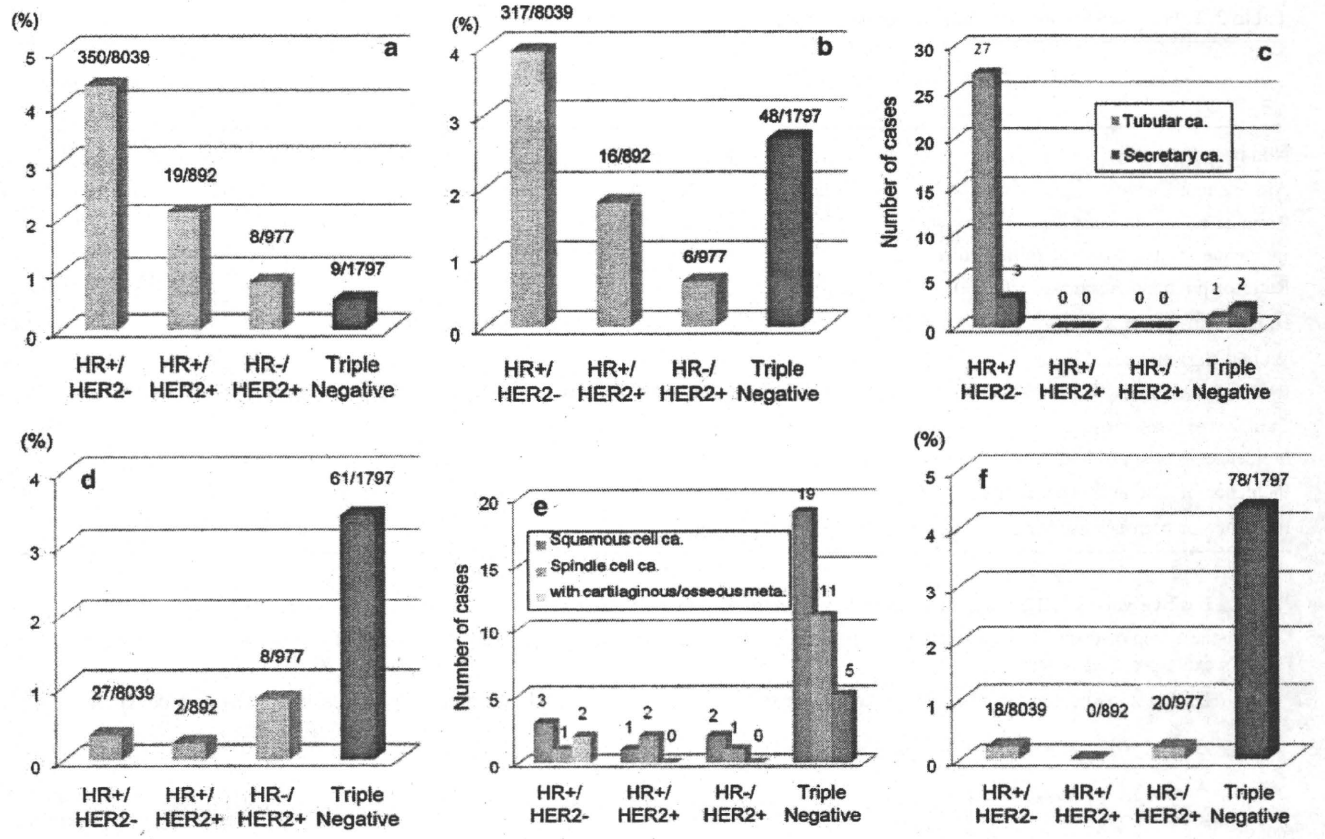

Fig. 4 **a** Incidence of mucinous carcinoma by receptor subtype. **b** Incidence of invasive lobular carcinoma by receptor subtype. **c** Incidence of tubular or secretary carcinomas by receptor subtype. **d** Incidence of medullary carcinoma by receptor subtype. **e** Incidence of metastatic carcinoma by receptor subtype. **f** Incidence of apocrine carcinoma by receptor subtype

Table 3 Chemotherapy according to receptor subtype

	Subtype			
	HR+/HER2−	HR+/HER2+	HR−/HER2+	TN
Number of cases	8,039	892	977	1,797
Node positive cases (%)	20.6	34.9	38.5	32.2
Number of patients treated by chemotherapy	3,913	696	940	1,563
Incidence of patients treated by ACR (%)	28.3	45.0	53.7	49.5
Incidence of patients treated by taxanes (%)	16.9	29.9	36.7	29.2
Incidence of neoadjuvant chemotherapy (%)	25.0	33.9	27.2	25.0

ACR anthracycline-containing regimen

regimens. In one patient there was a possibility that these two main regimens might have been administered concomitantly. ACR was administered to 28.3% of HR+/HER2− subtype tumors and taxane-based regimens to 16.9%. However, the incidence of axillary lymph nodes metastases was 20.6% in this subtype, which was smaller compared to other subtypes. In the other three subtype groups, as shown in Table 3, patients invariably received ACR or taxane regimens. Although the incidence of neoadjuvant chemotherapy was almost identical in each subtype group, the HR+/HER2+ group tended to be treated with this type of chemotherapy a little more frequently (Table 3).

Discussion

Of 14,749 breast cancer cases in Japan in 2004, 11,705 (79.4%) were examined for their ER, PgR, and HER2 status. TN tumors, defined as negative for all three receptors, accounted for 15.5% (1,819 cases). This was the largest collection of data on the prevalence rate of TN

tumors in Japan and was gathered from a large patient sample. Although there were no restrictions placed on the various centers for the methods they used for determining the presence of the receptors, or the criteria employed for their definition, we assumed that most cases had been examined using immunohistochemistry, since this technique for the detection of the receptors was in widespread use in 2004. It is possible that the hormone receptor status of some cases in this current study were incorrectly determined, because the definition criteria had not been established at that time in 2004. Most Japanese institutions regarded 0 or 2 on the Allred score as negative; others used a cutoff value of 10% for the determination of ER/PgR. Currently, the criteria for HER2 positivity are: 3+ with the IHC method, or 2+ with the IHC method and positive with the FISH method. However, in 2004, a tumor was defined as positive for HER2 if the IHC method resulted in 3+ alone, or in 2+ 3+.

Hence, in the present analyses, there were no strict criteria in place for the determination of ER, PgR, or HER2, leaving each institution to apply its own criteria. Now, however, it is considered that standardized analytical methods and definition criteria have been adopted nationwide, so that future analyses will be more reliable. Nevertheless, despite this limitation, we consider that the results of this population study are clinically very significant because of the large number of cases (over 11,000) and participating institutions (over 350).

The basal-like subtype accounts for 15–20% of breast cancers, irrespective of the method of analysis or ethnic group [6]. However, premenopausal African–American patients have a significantly higher incidence of this subtype compared to other patients [7, 11]. It is well known that the pathological and biological characteristics of breast cancer are significantly worse in young African–American patients and that they show a clinically poor prognosis. Therefore, the high incidence of basal-like subtype in young African–American patients correlates with the high histological grade of the tumors and the poor prognosis of the disease in this specific patient subgroup. On the other hand, it has been reported that this basal-like subtype is comparatively rare in Japanese women, with an incidence of only 8% documented in a recent study of 793 breast cancer cases in Japan [8]. We were interested in a possible familial nature of TN tumors, because of suggestions of a link to BRCA1 mutation. In the present study, however, we could not find any evidence of a family history of breast cancer in this subtype or that it affected younger women than other subtypes. This may have been due to the fact that various subtypes of breast cancer are included in the definition of 'TN,' although the basal-like subtype is thought to comprise 40–80% of cases [7, 12].

On the other hand, HR+/HER2− subtype tumors tended to be smaller and the patients freer of lymph node metastases at the time of diagnosis, while the HER2 subtypes were often positive for regional or distant lymph node metastases. This finding indicates the HR+/HER2− subtype tends to be detected at an earlier stage than the HR−/HER2+ subtype, which was characteristically diagnosed at an advanced stage. However, even if these tumors were both detected at an early stage, the difference in outcome would not be affected since HER2-positive tumors progress more rapidly.

Regarding histological subtypes, scirrhous carcinoma and solid-tubular carcinoma tended to be found more frequently in the HR+/HER2− and the TN subtypes, respectively. Although invasive lobular carcinoma was also found in the TN type, its true incidence is unclear as it is rarely difficult to distinguish from scirrhous carcinoma. This TN subgroup also included many cases of medullary and metaplastic carcinomas. Spindle cell and squamous cell carcinomas of the TN tumors showed metaplasia derived from invasive ductal carcinoma and exhibited characteristics of basal-like tumors [12]. However, medullary and apocrine carcinomas, which were included in the metaplastic carcinomas, have a better prognosis than the common type and, among TN breast cancers, should be regarded as different from the more common basal-like breast cancer.

There was no apparent correlation between the choice of chemotherapeutic regimen and tumor receptor subtype, both an anthracycline-containing regimen (ACR) and taxanes were used depending on the degree of progression. Neoadjuvant therapy was used in 27.2 and 25% of HR−/HER2+ and TN tumors, respectively, indicating that in 2004 this therapy was being used in large resectable tumors.

In conclusion, we analyzed data from a large number of breast cancer cases registered by the Japanese Breast Cancer Society in order to characterize and advance our understanding of the TN subtype of breast cancer. The present study demonstrated that it was important to establish standard analytical methods and criteria for detection of ER, PgR, and HER2 and that in particular it was necessary to define TN breast cancer more carefully. In the future, we need to follow up the prognosis and response to chemotherapy in these TN breast cancer cases in an attempt to characterize the subtype in more detail [2]. TN breast cancer simulates basal-like tumor, which has been classified from gene profiles. The basal-like type of TN breast cancer is diagnosed by IHC methods based on the expression of EGFR and cytokeratin 5/6. We are looking into further analyzing the cases from the 2004 registry from the perspectives of immunohistochemistry, prognosis, and use of adjuvant chemotherapy.

Acknowledgment We wish to thank Mr. Naohito Fukui, NPO Japan Clinical Research Support Unit. This work was supported by the research fund from the Japanese Breast Cancer Society.

Conflicts of interest statement. The author and his immediate family members open their conflicts of interest as follows: Employment: none; leadership: none; consultant: none; stock: none; honoraria: H. Iwase, AstraZeneca, Novartis; J. Kurebayashi, AstraZeneca, Takeda; research fund: H. Iwase, AstraZeneca, Taiho, Chugai, Takeda; testimony: none; other: none.

References

1. Bauer KR, Brown M, Cress RD, Parise CA, Caggiano V. Descriptive analysis of estrogen receptor (ER)-negative, progesterone receptor (PR)-negative, and HER2-negative invasive breast cancer, the so-called triple-negative phenotype: a population-based study from the California cancer Registry. Cancer. 2007;109:1721–8.
2. Carey LA, Dees EC, Sawyer L, Gatti L, Moore DT, Collichio F, et al. The triple negative paradox: primary tumor chemosensitivity of breast cancer subtypes. Clin Cancer Res. 2007;13:2329–34.
3. Nishimura R, Arima N. Is triple negative a prognostic factor in breast cancer? Breast Cancer. 2008;15:303–8.
4. Sorlie T, Perou CM, Tibshirani R, Aas T, Geisler S, Johnsen H, et al. Gene expression patterns of breast carcinomas distinguish tumor subclasses with clinical implications. Proc Natl Acad Sci USA. 2001;98:10869–74.
5. Sorlie T, Tibshirani R, Parker J, Hastie T, Marron JS, Nobel A, et al. Repeated observation of breast tumor subtypes in independent gene expression data sets. Proc Natl Acad Sci USA. 2003;100:8418–23.
6. Kobayashi S. Basal-like subtype of breast cancer: a review of its unique characteristics and their clinical significance. Breast Cancer. 2008;15:153–8.
7. Carey LA, Perou CM, Livasy CA, Dressler LG, Cowan D, Conway K, et al. Race, breast cancer subtypes, and survival in the Carolina Breast Cancer Study. JAMA. 2006;295:2492–502.
8. Kurebayashi J, Moriya T, Ishida T, Hirakawa H, Kurosumi M, Akiyama F, et al. The prevalence of intrinsic subtypes and prognosis in breast cancer patients of different races. Breast. 2007;16(Suppl 2):S72–7.
9. Harvey JM, Clark GM, Osborne CK, Allred DC. Estrogen receptor status by immunohistochemistry is superior to the ligand-binding assay for predicting response to adjuvant endocrine therapy in breast cancer. J Clin Oncol. 1999;17:1474–81.
10. Umemura S, Kurosumi M, Moriya T, Oyama T, Arihiro K, Yamashita H, et al. Immunohistochemical Evaluation for hormone receptors in breast cancer: a practically useful evaluation system and handling protocol. Breast cancer. 2006;13:232–5.
11. Millikan RC, Newman B, Tse CK, Moorman PG, Conway K, Dressler LG, et al. Epidemiology of basal-like breast cancer. Breast Cancer Res Treat. 2008;109:123–39.
12. Reis-Filho JS, Milanezi F, Steele D, Savage K, Simpson PT, Nesland JM, et al. Metaplastic breast carcinomas are basal-like tumours. Histopathology. 2006;49:10–21.

Abstract

INTERACTION OF LOW DOSE RADIATION AND OTHER FACTORS

Y. Shimada, M. Nishimura, Y. Amasaki, Y. Shang, K. Yamauchi, T. Sawai, S. Hirano, T. Imaoka, Y. Yamada, T. Takabatake, and S. Kakinuma*

It is well known that numerous factors can modify the dose response of cancer risk associated with radiation. These include age, gender, diet, genetic make-up, and environmental factors such as cigarette smoke and asbestos. Physical parameters such as radiation quality or LET (linear energy transfer), dose rate, and mode of fractionation also modify the effect of low-dose radiation. Precise risk assessment of low-dose radiation could be stepped forward by integrating the mechanistic approach with animal studies, which supplement epidemiological studies.

Children are more susceptible to radiation than adults (Preston et al. 2007). This is linked to more vigorous cell division during development, which results in the rapid fixation of DNA damage and clonal expansion of mutant cells. Specifically, the stem or progenitor cells, which are potential targets for carcinogenesis, or intestinal crypts, which have intestinal stem cells, increase in number by symmetric division in early life (Shimada et al. 1994). $Apc^{Min/+}$ mice, a model of human cancer syndrome of familial adenomatous polyposis, show highest susceptibility to x-ray-induced intestinal tumorigenesis at the neonatal stage (Okamoto and Yonekawa 2005). Induction of renal cell carcinoma in *Tsc2* heterozygous rats or hepatocarcinoma in B6C3F1 mice by irradiation is most efficient at the perinatal stage (Kokubo et al. 2010). Interestingly, the progenitor cells during development show distinct response to radiation from this sector in adult cells. The National Institute of Radiological Science (NIRS) has begun a project on the cancer susceptibility of breast, lung, colon, liver, brain, and kidney and hematopoietic neoplasm from early life radiation exposure.

The human population is heterogenous in radiosensitivity and includes a number of sensitive subpopulations. The defects are associated with DNA damage response; i.e., cell cycle checkpoint and DNA repair such as RB, TRP53, ATM, and BRCA1/2. Survivors of hereditary retinoblastoma are known to have an elevated risk of secondary cancers of bones, soft tissue, and brain after radiotherapy. Deficiency in DNA-PKcs, which plays a crucial role in V(D)J recombination in lymphocytes and non-homologous end-joining repair, results in an increased incidence of thymic lymphoma in mice at 250 mGy. The defects in the genes involved in the development or signal transduction are also associated with increased susceptibility. Nevoid basal cell carcinoma syndrome patients, who have defective *PTCH* gene, are extremely sensitive to the carcinogenic effect of ionizing radiation (Scharnagel and Pack 1949). A murine model of *Ptc1* heterozygous mice can be induced with medulloblastomas by x-rays at 100–250 mGy. Age at postnatal day 1–4 is the most susceptible period, and the sensitivity decreases thereafter.

Genetic background modifies radiation-induced cancer. *Ptc1* heterozygous mice with CD1 background show high tumor response, but those with C57BL/6 background are completely non-responsive (Pazzaglia et al. 2006). Multiplicity of intestinal tumors in $Apc^{Min/+}$ is modulated by mouse strains in the order of C3B6 > B6 > CB6 > A/JB6. However, multiplicity of mammary tumors in $Apc^{Min/+}$ is not influenced by genetic background.

Because human cancers are caused mainly by non-radiogenic sources such as cigarette smoke and food, the effect of radiation is a result of combined exposure to these substances. Low dose-rate irradiation or repeated small doses of radiation exposure reduces chemically-induced carcinogenesis (Sasaki 1991). Surprisingly, the low-dose radiation suppresses not only the induction of mutation by the ENU mutagen but also subsequent clonal expansion of mutants (Yamauchi et al. 2007). On the

* Experimental Radiobiology for Children's Health Research Group, National Institute of Radiological Sciences, 4-9-1 Anagwa, Inage-ku, Chiba 263-8555 Japan.

For correspondence contact Yoshiya Shimada at the above address, or email at y_shimad@nirs.go.jp.

(*Manuscript accepted* 22 *November* 2010)
0017-9078/10/0

DOI: 10.1097/HP.0b013e3182080e07

other hand, combination with high dose radiation (1 Gy) enhances mutant frequency in a synergistic manner.

Identification of radiation signature in tumors may have an impact on the application for attributable risk in human population exposed to low-dose radiation. Radiation-induced mouse thymic lymphoma shows a high frequency of interstitial deletion at *Ikaros* locus, which is much less frequently observed in spontaneously developed or alkylating-agent induced lymphoma (Shimada et al. 2000; Kakinuma et al. 2005; Takabatake et al. 2008). Loss of wild-type *Apc* allele typically results from loss of the entire chromosome 18 in spontaneous intestinal tumors of $Apc^{Min/+}$, while that in radiation-induced tumors is of the interstitial type (Luongo 1996). In spontaneous medulloblastoma, *Ptc1* LOH occurs through loss of distal region in chromosome 13 , but tumors in irradiated mice have interstitial LOH (Pazzaglia et al. 2006). Interestingly, the frequency of LOH increases as a function of dose and is significant in tumors induced by 50 mGy (Takabatake et al. 2008). Health Phys. 100(3):278–279; 2011

Key words: cancer; dose, low; health effects; radiation dose

REFERENCES

Kakinuma S, and others. Frequent retention of heterozygosity for point mutations in p53 and Ikaros in N-ethyl-N-nitrosourea-induced mouse thymic lymphomas. Mutation Research 572:XXX-XXX; 2005.

Kokubo T, and others. Age dependence of radiation-induced renal cell carcinomas in an Eker rat model. Cancer Science 101:8; 2010.

Luongo C. Somatic genetic events linked to the Apc locus in intestinal adenomas of the Min mouse. Genes Chromosomes Cancer 17:5; 1996.

Okamoto M, Yonekawa H. Intestinal tumorigenesis in Min mice is enhanced by x-irradiation in an age-dependent manner. J Radiat Res 46:9; 2005.

Pazzaglia S, and others. Two-hit model for progression of medulloblastoma preneoplasia in patched heterozygous mice. Oncogene 25:6; 2006.

Preston DL, and others. Solid cancer incidence in atomic bomb survivors. Radiat Research 168:64; 2007.

Sasaki S. Influence of the age of mice at exposure to radiation on life-shortening and carcinogenesis. J Radiat Research 213; 1991.

Scharnagel IM, Pack GK. Multiple basal cell epitheliomas in a 5-y-old child. Am J Diseases Children 77:5; 1949.

Shimada Y, and others. Age and radiation sensitivity of rat mammary clonogenic cells. Radiat Research 137:6; 1994.

Shimada Y, and others. Radiation-associated loss of heterozygosity at the Znfn1a1 (Ikaros) locus on chromosome 11 in murine thymic lymphomas. Radiat Research 154:8; 2000.

Takabatake T, and others. Analysis of changes in DNA copy number in radiation-induced thymic lymphomas of susceptible C57BL/6, resistant C3H and hybrid F1 Mice. Radiat Research 169:11; 2008.

■ ■

Carcinogenesis vol.31 no.9 pp.1694–1701, 2010
doi:10.1093/carcin/bgq145
Advance Access publication July 8, 2010

Genomic and gene expression signatures of radiation in medulloblastomas after low-dose irradiation in *Ptch1* heterozygous mice

Yuka Ishida[1,2,†], Takashi Takabatake[3,†], Shizuko Kakinuma[3], Kazutaka Doi[4], Kazumi Yamauchi[3], Mutsumi Kaminishi[3], Seiji Kito[5], Yuki Ohta[5,6], Yoshiko Amasaki[3], Hiroyuki Moritake[6], Toshiaki Kokubo[1,2], Mayumi Nishimura[3], Tetsu Nishikawa[1], Okio Hino[2] and Yoshiya Shimada[3,*]

[1]Department of Technical Support and Development, Fundamental Technology Center, National Institute of Radiological Sciences, 4-9-1 Anagawa, Inage-ku, Chiba 263-8555, Japan, [2]Department of Molecular Pathogenesis, Juntendo University, 2-1-1 Hongo, Bunkyo-ku, Tokyo 113-8421, Japan, [3]Experimental Radiobiology for Children's Health Research Group, Research Center for Radiation Protection, National Institute of Radiological Sciences, 4-9-1 Anagawa, Inage-ku, Chiba 263-8555, Japan, [4]Regulatory Sciences Research Group, Research Center for Radiation Protection, National Institute of Radiological Sciences, 4-9-1 Anagawa, Inage-ku, Chiba 263-8555, Japan, [5]Department of Advanced Technologies for Radiation Protection Research, Research Center for Radiation Protection, National Institute of Radiological Sciences, 4-9-1 Anagawa, Inage-ku, Chiba 263-8555, Japan and [6]Science Service, Inc., 2-7, Nihombashi Ohdemma-cho, Chuo-ku, Tokyo 103-0011, Japan

*To whom correspondence should be addressed. Tel: +81 43 206 3200; Fax: +81 43 206 4138;
Email: y_shimad@nirs.go.jp

Accurate cancer risk assessment of low-dose radiation poses many challenges that are partly due to the inability to distinguish radiation-induced tumors from spontaneous ones. To elucidate characteristic features of radiation-induced tumors, we analyzed 163 medulloblastomas that developed either spontaneously or after X-ray irradiation at doses of 0.05–3 Gy in *Ptch1* heterozygous mice. All spontaneous tumors showed loss of heterozygosity in broad regions on chromosome 13, with losses at all consecutive markers distal to *Ptch1* locus (S-type). In contrast, all tumors that developed after 3 Gy irradiation exhibited interstitial losses around *Ptch1* with distal markers retained (R-type). There was a clear dose-dependent increase in the proportion of R-type tumors within the intermediate dose range, indicating that the R-type change is a reliable radiation signature. Importantly, the incidence of R-type tumors increased significantly ($P = 0.007$) at a dose as low as 50 mGy. Integrated array-comparative genomic hybridization and expression microarray analyses demonstrated that expression levels of many genes around the *Ptch1* locus faithfully reflected the signature-associated reduction in genomic copy number. Furthermore, 573 genes on other chromosomes were also expressed differently between S-type and R-type tumors. They include genes whose expression changes during early cerebellar development such as *Plagl1* and *Tgfb2*, suggesting a recapitulation of gene subsets functioning at distinct developmental stages. These findings provide, for the first time, solid experimental evidence for a significant increase in cancer risk by low-dose radiation at diagnostic levels and imply that radiation-induced carcinogenesis accompanies both genomic and gene expression signatures.

Introduction

During the last decade, diagnostic use of radiation has dramatically increased by as much as 2- to 3-fold in many countries. Despite the clear benefits of diagnostic radiation, the potential for increased cancer risk, particularly in children, is alarming (1–5). International and domestic regulatory organizations for radiation protection recommend the use of the so-called 'linear no-threshold' model (6,7), in which cancer risk from low doses (<100 mSv) is extrapolated from the risk from moderate to high doses using the hypothesis of a linear dose–response relationship. Epidemiological studies indeed provide evidence for increased cancer risk at low doses (8–12). However, whether cancer risk following low doses fits the linear no-threshold model is still controversial. A mechanistic understanding of carcinogenesis induced by low-dose radiation is required for accurate estimation of cancer risk following exposure to low doses (13).

There is considerable variation in radiation-induced cancer susceptibility among humans, and genetic susceptibility to spontaneous tumors is accompanied by a greater-than-normal risk after radiation (14). Cancer-prone subpopulations include those who have genetic defects in DNA repair or developmental signaling pathways, such as the Hedgehog and Wnt pathways (15). Inherited inactivation of Ptch1, the sonic hedgehog (Shh) receptor and a negative regulator of the pathway (16,17), predisposes humans to childhood tumors such as medulloblastoma (MB) and rhabdomyosarcoma, as well as adult tumors such as basal cell carcinoma, also known as Gorlin syndrome (18). Gorlin syndrome patients are sensitive to the carcinogenic effect of radiation (19). The *Ptch1* heterozygous mouse is an established model of human Gorlin syndrome (20,21). Pazzaglia *et al.* (22,23) reported important findings for risk assessment of MB using $Ptch1^{+/-}$ mice. They showed a significant effect of intermediate doses of radiation (250 and 500 mGy), with an increase in MB incidence and a shortening of mean survival time in $Ptch1^{+/-}$ mice on the CD1 background (22). Furthermore, they revealed that distinct chromosomal inactivation mechanisms were responsible for *Ptch1* loss in spontaneous versus high-dose radiation-induced MB (23).

To elucidate the cancer risk following low-dose radiation at <100 mGy, we irradiated newborn C3B6F1 $Ptch1^{+/-}$ mice and examined the dose dependency of MB induction and the underlying molecular mechanism. We show that MB incidence increased and latency shortened even with an exposure of 50 mGy, which is comparable with the dose received from a computed tomography scan. Consistent with a previous report (23), we found that radiation-induced tumors can be clearly distinguished from spontaneous tumors by the mode of loss of wild-type *Ptch1*. Radiation-associated *Ptch1* loss was mediated by interstitial deletion, and spontaneous loss was mediated by mitotic recombination or non-disjunction with a subsequent duplication. Radiation-induced *Ptch1* deletion increased in a dose-dependent manner, thus indicating that *Ptch1* deletion is a useful radiation signature for evaluating the effects of low-dose radiation on carcinogenesis. Furthermore, this genomic radiation signature enabled us to identify many genes whose expression differed significantly between tumors having or lacking the signature. Some of these genes were located on chromosome 13 (chr-13), and their expression levels faithfully reflected the signature-associated genomic copy number reduction. Other genes were located on other chromosomes and included genes involved in early development of cerebellar granule neuron precursors, an origin for Shh pathway-associated MB (24). These findings further our understanding of the risk of carcinogenesis following low-dose radiation, including exposure from medical diagnostic tests given to patients genetically predisposed for cancer; our results also suggest underlying mechanisms for radiation-induced carcinogenesis.

Abbreviations: array-CGH, array-based comparative genomic hybridization; chr-6, chromosome 6; chr-13, chromosome 13; IR, ionizing radiation; LOH, loss of heterozygosity; MB, medulloblastoma; PCR, polymerase chain reaction; PN, postnatal day; Shh, sonic hedgehog.

[†]These authors contributed equally to this work.

Materials and methods

Mice

All animals were bred under conventional conditions in our animal facility. Mice lacking one *Ptch1* allele ($ptc^{neo67/+}$), generated by disruption of exons

6 and 7 in 129S2 ES cells (21), were obtained from the European Mouse Mutant Archive (http://www.emmanet.org/), where they had been backcrossed to C57BL/6 mice for three generations. They were then bred for four generations to C57BL/6JCrl mice in our laboratory. F1 hybrid mice generated by crossing C3H/He females and C57BL/6$^{Ptch1+/-}$ males (the latter obtained from *in vitro* fertilized embryos) were assigned to eight groups: non-irradiated controls and seven dose groups for X-ray irradiation. All animal experiments were conducted according to legal regulations in Japan and were carried out with permission and under regulation of the Institutional Animal Care and Use Committee of National Institute of Radiological Sciences.

X-ray irradiation

Ptch1$^{+/-}$ mice and wild-type littermates were irradiated at postnatal day (PN) 1 at dose rates of ~0.65 Gy/min (for total doses >0.1 Gy) or ~0.10 Gy/min (for total doses ≤0.1 Gy). Irradiation was performed using a Pantak HF-320 X-ray generator (Pantak Ltd, East Haven, CT).

Tissue preparation

Ptch1$^{+/-}$ mice were observed daily until moribund (i.e. marked emaciation, ruffling of fur or inactivity) and then were euthanized by venesection under ether anesthesia. *Ptch1*$^{+/-}$ mice that were still alive at the end of the observation period (PN250) were also euthanized. Portions of cerebellar tumors and normal tissue (ear and tail) were snap frozen in liquid nitrogen. The remaining whole brains were fixed with 10% neutral-buffered formalin. These specimens were embedded in paraffin to prepare coronal or sagittal sections, which were stained with hematoxylin and eosin.

Extraction of genomic DNA and total RNA

For loss of heterozygosity (LOH) analysis, genomic DNA was isolated from MBs and ear samples using the Maxwell 16 Instrument and System (Promega, Madison, WI). For microarray analyses, genomic DNA and total RNA were purified using an AllPrep DNA/RNA Mini Kit (Qiagen, Valencia, CA) and Trizol Reagent (Invitrogen, Carlsbad, CA). Briefly, samples were homogenized in Buffer RLT plus buffer included in the kit, and genomic DNA was isolated using an AllPrep DNA spin column followed by RNase treatment. To prepare RNA samples, the homogenates were diluted 10-fold with Trizol Reagent, and total RNA was subsequently purified. The quality of total RNA was assessed using the QIAxcel system (Qiagen).

LOH analysis

Genomic DNA was amplified by polymerase chain reaction (PCR) using the following polymorphic markers: *D13Mit303*, *D13Mit91*, *D13Mit210*, *D13Mit159*, *D13Mit76* and *D13Mit35*. PCR products were resolved with the capillary electrophoretic system HDA-GT12 Genetic analyzer with a Gel Cartridge Kit GSK-5000F (eGene, Irvine, CA). LOH analysis at the *Ptch1* locus was also performed according to Pazzaglia *et al.* (23) by determining the sequence of exon 23, which includes a T/C polymorphism at position 4016 of the *Ptch1* locus. All LOH analyses were performed on genomic DNAs from tumors and corresponding genomic DNAs from normal ear tissue as a control.

Array-based comparative genomic hybridization analysis

We designed and used Agilent 8 × 15 K-formatted and 4 × 44 K-formatted mouse custom array-based comparative genomic hybridization (array-CGH) microarrays. Oligonucleotide probes in these custom microarrays distributed unevenly across the murine genome, with relatively higher densities in regions of interest including the region around *Ptch1*. Fluorescent labeling of DNA, microarray hybridization and post-hybridization washing were carried out according to the manufacturer's protocol (version 5) for oligonucleotide array-CGH for genomic DNA analysis (Agilent Technologies, Santa Clara, CA). Scanning was performed using an Agilent microarray scanner (G2565BA; Agilent Technologies). Signal intensities were measured with Feature Extraction software v9-5-1 and were evaluated using DNA analytics software v4-0-81 (Agilent Technologies).

Expression microarray analysis

For each analysis, 800 ng of total RNA was amplified and labeled with Cyanine 3 using Agilent's Low RNA Input Linear Amplification Kit (Agilent Technologies) following the manufacturer's protocol (version 5.5). Hybridization was performed on Whole Mouse Genome oligonucleotide microarrays (Agilent G4122F) using reagents and protocols provided by the manufacturer. Microarray data were analyzed using GeneSpring GX 10.0.2 (Agilent Technologies). Expression data were normalized both 'per chip' to the 75th percentile of all measurements in that sample and 'per gene' to the median expression levels of the gene across all samples except otherwise indicated. To remove probes with unreliable expression measurements, probes were filtered based on their signal intensity values and flag values. One-way analysis of variance was performed using Benjamini and Hochberg's false discovery rate as the multiple testing correction, with a *P*-value cut-off of 0.05. The microarray data reported in this article have been deposited in the Gene Expression Omnibus database at www.ncbi.nlm.nih.gov/geo (accession no. GSE19384). Affymetrix GeneChip microarray data on expression profiles of the developing cerebellum during PN days 1–21, which were part of data deposited in the Gene Expression Omnibus database by Kho *et al.* (accession no. GSE14514), were utilized by importing Affymetrix CEL files into GeneSpring GX 10.0.2. Data were processed with the summarization algorithm of Robust Multichip Analysis, and the baseline was transformed with respect the median of all samples.

Quantitative reverse transcription–PCR analysis

First strand complementary DNA was synthesized from 2 μg of total RNA using ReverTra Ace (Toyobo, Tokyo, Japan). The quantitative PCR reaction was performed on an Mx3000P real-time PCR system (Agilent Technologies) by using Premix Ex Taq (Takara Bio, Shiga, Japan) for the expression of a housekeeping gene, *Gapdh*, and by using SYBR Premix Ex Taq (Takara Bio) for the expression of *Plagl1* and *Tgfb2*. The primer sequences used are listed in supplementary Table I, available at *Carcinogenesis* Online. The PCR program consisted of denaturation at 95°C for 10 s and 45 subsequent amplification cycles of denaturation at 95°C for 5 s and annealing/elongation at 60°C for 20 s. Relative gene expression was calculated by the $2^{-\Delta\Delta C}{}_{T}$ method (25).

Statistical analysis

To assess the dose-dependent effects of radiation on the incidence of MB, we used a Cox proportional hazard model to compute hazard ratios of each dose group relative to the non-irradiated group. We also assessed the linear increase in incidence according to the dose. We compared survival time between mice with S-type and R-type tumors by a Cox regression model, and the results were presented in terms of the hazard ratio. To adjust for radiation dose, this analysis was stratified by dose groups. In addition, we compared the proportion of R-type tumors between non-irradiated and 50 mGy irradiated groups with a Mantel–Haenszel test, which was stratified by gender. These analyses were performed using SAS version 9.2 (SAS Institute, Cary, NC).

Results

Dose-dependent increase of MB incidence in Ptch1 heterozygous mice following irradiation

To examine dose-dependent effects of radiation on MB development, we irradiated *Ptch1*$^{+/-}$ mice on the C3B6F1 background at PN1, when mice are most susceptible to the carcinogenic actions of ionizing radiation (IR) (22), and followed their survival until 250 days of age. As shown in supplementary Table II, available at *Carcinogenesis* Online, we found that *Ptch1*$^{+/-}$ mice showed a high incidence of spontaneous MB (34.5% at 250 days of age). The effects of radiation were observed even in mice exposed to low doses of 50 and 100 mGy (Figure 1; supplementary Table II is available at *Carcinogenesis* Online). There was a significant dose-dependent increase in the incidence rate of MB ($P < 0.0001$), indicating a dose-dependent shortening of the latent period. The mean survival time of mice that died due to MB before 250 days of age was shortened with increasing radiation doses (supplementary Table II is available at *Carcinogenesis* Online). Although the increase in the rate of MB was not statistically significant in mice receiving the lowest dose (50 mGy) compared with non-irradiated mice, the rate was significantly higher in mice exposed to higher doses (supplementary Table III is available at *Carcinogenesis* Online).

Dose-dependent increase of interstitial allelic losses of the genomic region around Ptch1

Pazzaglia *et al.* (23) suggested that the pattern of LOH on chr-13 in six radiation-induced (3 Gy) MBs may be distinguished from that in four spontaneous MBs that developed in *Ptch1*$^{+/-}$ mice. We thus examined patterns of chr-13 LOH in all tumors for which both tumor and normal ear DNAs were available using six microsatellite markers (Figure 2; supplementary Figure 1A is available at *Carcinogenesis* Online). We observed that 146 of 163 (90%) MBs showed loss of the C3H-derived wild-type allele at one or more of the six markers. These 146 tumors were grouped into two types: S-type tumors showed LOH in broad regions on chr-13, with losses at all consecutive markers distal to *Ptch1* locus, and R-type tumors showed interstitial losses around the *Ptch1* locus with distal markers retained. We then

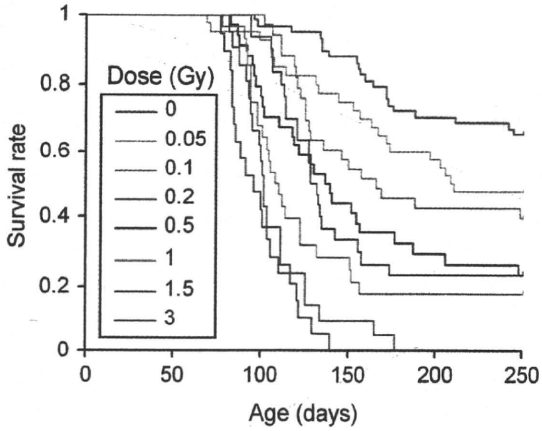

Fig. 1. Survival curves showing dose-dependent effects of radiation in *Ptch1* heterozygous mice. Irradiation was carried out at PN1. *Ptch1*$^{+/-}$ mice were monitored for 250 days. The life span of mice irradiated with doses ≥0.1 Gy was significantly shorter compared with non-irradiated control mice ($P < 0.05$).

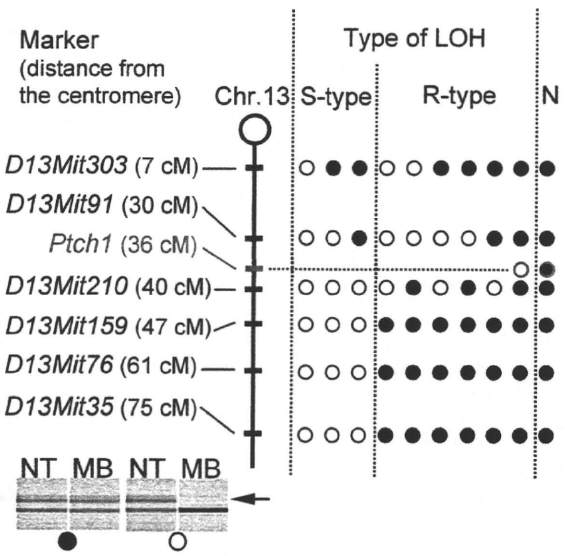

Fig. 2. Analysis of chr-13 LOH in spontaneous and radiation-induced MBs from *Ptch1*$^{+/-}$ mice. Polymorphic markers and their positions indicating distances (cM) from the centromere are shown on the left of the schematic chromosome. Representative electrophoretic profiles for normal tissue (NT; ear) and tumors (MB) are shown at the bottom left, indicating retention of both alleles (closed circles) and loss of the wild-type C3H allele (open circles), which is indicated by an arrow. S-type: allelic loss observed at all consecutive markers distal to *Ptch1* locus. R-type: allelic loss only at interstitial markers with distal markers retained or at position 4016 of *Ptch1*. Another case with a small intragenic deletion within the *Ptch1* locus was also included in this type. N: two tumors that showed neither LOH nor copy number reduction on chr-13.

examined whether the remaining 17 MBs showed LOH at the *Ptch1* locus by exploiting a T/C polymorphism at position 4016 of *Ptch1* (23). Of these MBs, 14 showed loss of the wild-type C3H allele (supplementary Figure 1B is available at *Carcinogenesis* Online). The remaining three tumors were further analyzed by array-CGH, which revealed that one MB had an intragenic microdeletion (~7.9 kb) in the region slightly more telomeric to the above-mentioned T/C polymorphism (supplementary Figure 1C and D is available at *Carcinogenesis* Online). We did not detect a loss of the wild-type *Ptch1* allele in the remaining two MBs. This microdeletion and the above-mentioned 14 tumors were classified as R-type. Thus, we identified aberrations on chr-13 in 161 of 163 (99%) tumors analyzed, a result that is consistent with Knudson's two-hit theory (26,27). Notably, all 19 spontaneous MBs were classified as S-type, whereas all 19 MBs induced after 3 Gy irradiation had R-type LOH patterns (Table I). The incidence of R-type tumors was dose dependent and, importantly, R-type tumors were found even in mice exposed to the lowest radiation dose (50 mGy; Figure 3A and B). These data strongly demonstrated that an R-type LOH pattern can be considered a reliable radiation signature. The proportion of R-type patterns was significantly different in mice exposed to the lowest dose (50 mGy) compared with non-irradiated mice ($P = 0.0071$, Mantel–Haenszel test). We also noticed that the distribution of survival time of R-type MBs (red diamonds in Figure 3A) appeared to be shifted downwardly compared with that of S-type MBs (light blue diamonds in Figure 3A), suggesting that R-type MBs had relatively shorter latent periods as a whole. Statistical analysis indicated that R-type MBs had greater risk of death than S-type MBs (hazard ratio, 1.64; 95% confidence interval 1.05–2.57). In association with this, we analyzed whether there were histological differences between S-type and R-type MBs, as well as those between MBs with short and long latencies. Although focal areas of tumors occasionally showed desmoplastic reaction in some cases, majority of MBs showed anaplastic cells or monomorphic round cells, and no clear differences which were associated either with the type of LOH (S- or R-type) or length of latency were observed.

Interstitial chr-13 deletions in MBs revealed by array-CGH analysis

To characterize S-type and R-type tumors in more detail, we performed array-CGH analysis on 12 tumors. S-type tumors were selected from tumors that developed in non-irradiated control mice or mice exposed to 0.2 Gy irradiation, and R-type tumors were selected from mice that received 0.2 or 1.5 Gy irradiation (three per group; supplementary Table IV is available at *Carcinogenesis* Online and Figure 4A). Array-CGH analysis revealed a copy number reduction at a small region within *Ptch1*, which included exons 6 and 7, in all 12 MBs analyzed (Figure 4A). Because the genomic region containing exons 6 and 7 was replaced with a neomycin resistance cassette (21), loss of this region indicated a loss of the maternal wild-type C3H allele of *Ptch1*. Although all S-type MBs showed normal copy numbers in other regions throughout chr-13 independent of LOH status, R-type MBs showed a 2-fold reduction in copy number in all interstitial regions exhibiting loss of the C3H allele (Figure 4A). These data suggest that S-type LOH patterns resulted from a mitotic recombination or a non-disjunction with a subsequent duplication, whereas R-type patterns may have resulted from interstitial deletion.

Strong association between gene expression and genomic copy number aberrations

We next carried out microarray gene expression analysis on the same 12 MBs to examine how expression profiles differed among MBs in connection with the dose of radiation and mode of *Ptch1* loss. Gene expression patterns in normal cerebellum at comparable ages (103–113 days after birth) were also analyzed for reference (supplementary Table IV is available at *Carcinogenesis* Online). Using principal component analysis, we observed that the six R-type MBs formed a readily discernible assembly (Figure 4B), suggesting that R-type MBs were highly similar with respect to gene expression. To identify genes whose expression was significantly different between groups, we performed one-way analysis of variance with Tukey's post-hoc test. This analysis identified 1183 genes (1297 probes) whose expression differed between the four groups. The result of the Tukey's post-hoc test indicated that the majority of the genes were differentially expressed between S-type and R-type MBs (supplementary Table V is available at *Carcinogenesis* Online). Among them, 95 genes (141 probes) were located within the common deleted region around the *Ptch1* locus on chr-13 in the six R-type MBs. Most of the genes revealed expression that was reduced almost by half in R-type MBs, suggesting that the expression faithfully reflected copy

number reduction. Figure 4C shows expression levels revealed by 1188 probes (818 genes), which were mapped on chr-13. The light blue regions, which are rich in genes with decreased expression, coincided accurately with the deleted regions shown in Figure 4A. Of note, the expression level of *Ptch1* was also decreased by copy number reduction (Figure 5A). Although the expression of *Shh* in all tumors was below measurable levels, three other hedgehog targets and mediator genes (*Ptch2*, *Gli1* and *Gli2*) were upregulated to a similar extent in all tumors (Figure 5B–D), perhaps reflecting constitutive activation of the Hedgehog/Patched signaling pathway due to inactivation of both *Ptch1* alleles.

Association between the radiation signature and early-PN development of the cerebellum

The mode of *Ptch1* loss also significantly affected hundreds of genes located on chromosomes other than chr-13. Comparison of genes found to be differentially expressed between groups based on Tukey's post-hoc test (supplementary Table V is available at *Carcinogenesis* Online) revealed that 573 genes (664 probes) located on chromosomes other than chr-13 showed differential expression in all cases of comparison between groups of S-type and R-type tumors. Interestingly, these genes included *Plagl1/Zac1* and *Tgfb2*, which are reported to be strongly expressed transiently during early development of cerebellar granule cell (28,29). The quantitative reverse transcription–PCR analysis on the expression of *Plagl1/Zac1* and *Tgfb2* validated the microarray data; transcriptional level of *Plagl1/Zac1* was much higher in R-type than S-type, whereas that of *Tgfb2* was higher in S-type than R-type (Figure 5E and F). The statistical significance of their different expression levels between S-type and R-type MBs was still maintained after the data of additional six S-type and nine R-type MBs (supplementary Table IV is available at *Carcinogenesis* Online) were included for analysis. Because the peak expression of *Plagl1/Zac1* (28) occurs at earlier developmental stages than that of *Tgfb2* (29), global gene expression of R-type MBs might be associated with earlier developmental stages of cerebellum. It is of note that global gene expression within individual MBs reflects particular stages of cerebellar development (30). Next, we examined whether there was an association between the 573 differentially expressed genes and certain stages of the developing cerebellum. These 573 genes were subdivided into two groups based on whether they were expressed higher in R-type or S-type tumors (supplementary Figure 2A and B is available at *Carcinogenesis* Online). Based on microarray data on the expression profiles of the developing cerebellum during PN1–PN21 [as deposited in the Gene Expression Omnibus database by Kho *et al.* (30)], we selected genes that were included in that database and whose expression changed >1.5-fold or 2-fold during PN1–PN21. The histograms in supplementary Figure 2C and D (available at *Carcinogenesis* Online) represent the number of probe sets as a function of the day when the intensity of the probe set was maximal. Many genes whose expression was higher in R-type tumors showed maximum expression at PN1–PN5 (supplementary Figure 2C is available at *Carcinogenesis* Online), suggesting an association between the radiation signature and the early stages of PN cerebellar development.

Table I. Dose-dependent increase in the proportion of R-type tumors

Dose (Gy)	Number of analysis	S-type	R-type	N^a
0	19	19 (100.0)	0 (0.0)	0
0.05	20	13 (65.0)	7 (35.0)	0
0.1	19	9 (47.4)	9 (47.4)	1
0.2	22	9 (40.9)	13 (59.1)	0
0.5	23	6 (26.1)	17 (73.9)	0
1	20	2 (10.0)	18 (90.0)	0
1.5	21	3 (14.3)	17 (81.0)	1
3	19	0 (0.0)	19 (100.0)	0

[a]Number of tumors that showed neither LOH nor copy number reduction on chr-13.

Association between frequent aneuploidy of chromosome 6 and gene expression

Besides deletions on chr-13, aneuploidies of chromosome 6 (chr-6) and the X chromosome were prominent aberrations (supplementary Table VI is available at *Carcinogenesis* Online). The correlation between expression levels of genes on chr-6 and their genomic dosage was examined (supplementary Figure 3 is available at *Carcinogenesis* Online). It was found that expression levels of many genes on chr-6 reflected aneuploidy of chr-6. Among 2161 probes (1494 genes) on chr-6 analyzed, 835 probes (534 genes) revealed increased expression as a function of genomic dosage of chr-6 (Pearson correlation coefficient > 0.5). Supplementary Figure 3C (available at *Carcinogenesis* Online) shows the correlation of the 10 genes with the highest coefficients, together with that of *FoxM1* (0.90) and *Ccnd2* (0.76), which were suggested as potential candidate genes on chr-6 that contribute to tumorigenesis of MB in relationship with trisomy 6 (31) or partial amplification of chr-6 (32).

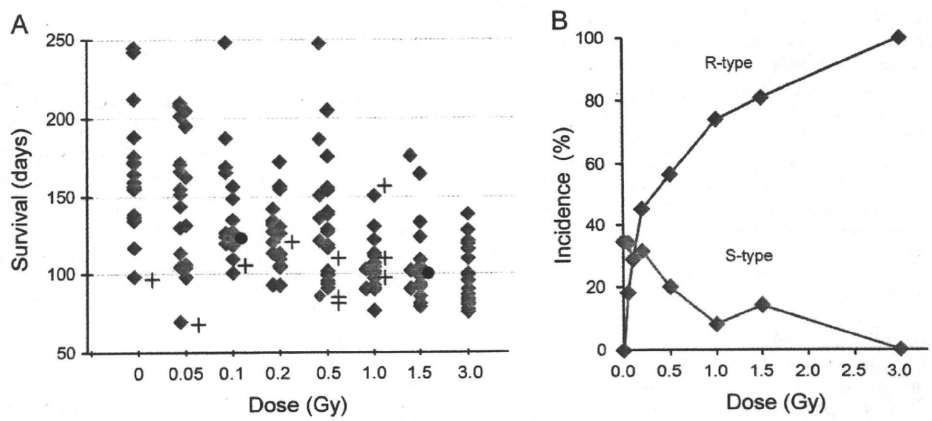

Fig. 3. Relationship between survival of individual tumor-bearing mice and chr-13 LOH pattern. (**A**) Light blue and red diamonds represent mice with S-type and R-type tumors, respectively. Two black circles at doses of 0.1 and 1.5 Gy correspond to tumors that showed neither LOH nor copy number reduction on chr-13. Crosses indicate mice whose MB DNAs could not be used for LOH analysis. (**B**) Dose-effect relationships of the incidence of S-type (light blue diamonds) and R-type (red diamonds) tumors. Some tumors could not be examined for LOH analysis due to the absence of frozen tumor samples. Therefore, we calculated the incidence of S-type and R-type tumors by multiplying the total MB incidence at each dose by the rate of both tumor types, of which LOH could be determined. The shape of the dose–response curve of R-type tumor incidence is downwardly concave in the 0–3 Gy dose range, and the linear relationship is not rejected when the goodness of fit is assessed in the 0–0.2 Gy dose range by the chi-square test ($P = 0.13$).

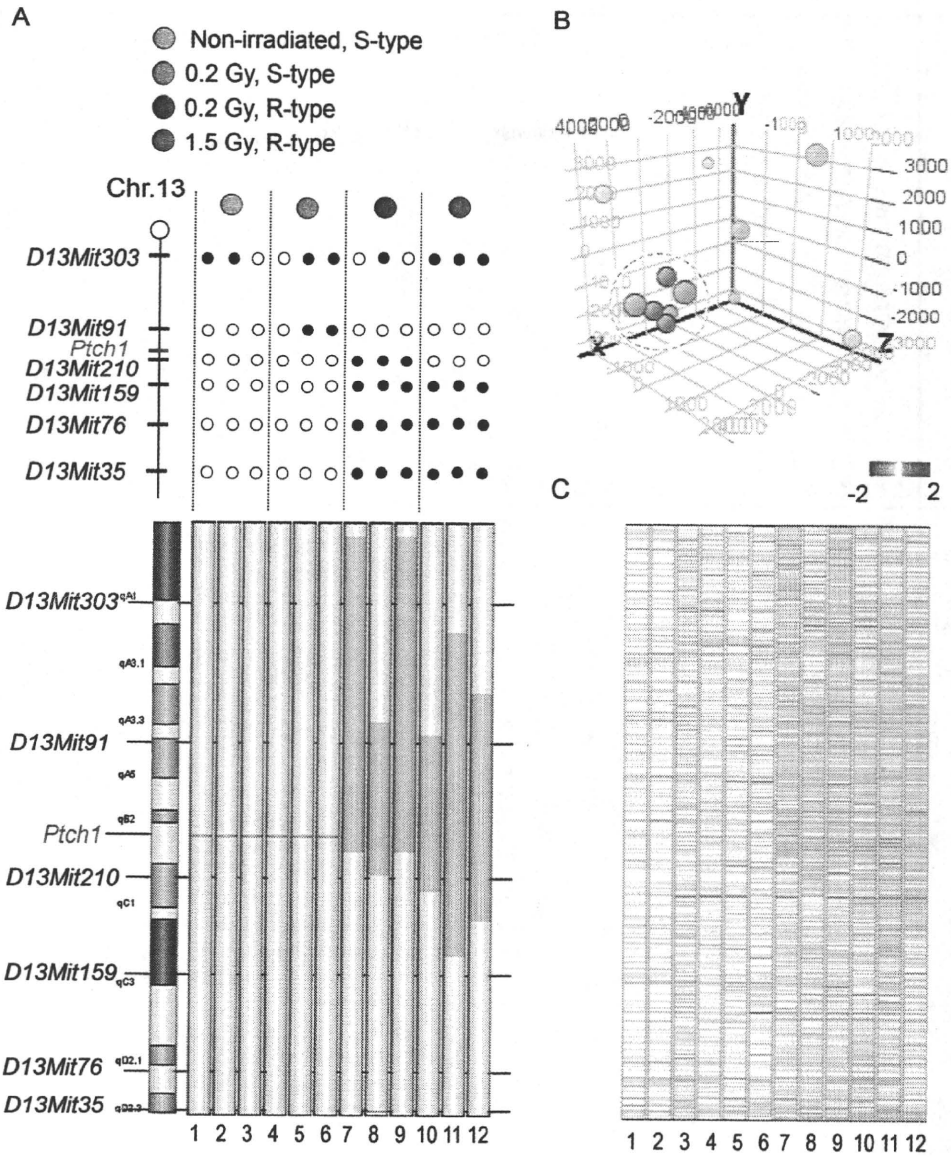

Fig. 4. Strong association between gene expression and copy number reduction on chr-13. (**A**) Twelve MBs were analyzed from four different subgroups of three MBs each and are represented by colored circles as illustrated at the top. LOH patterns of tumors are shown in the middle. Open circles and closed circles indicate loss of the C3H allele and retention of both alleles, respectively. Deleted regions detected by array-CGH analysis are shown in green at the bottom. As for the deletions in two R-type tumors (S14586, no.8 and S14862, no.12), the sequence of the break points could be determined (supplementary Figure 1D is available at *Carcinogenesis* Online) after PCR amplification of the region containing the break points. (**B**) Principal component analysis plot of gene expression profiles of all 12 tumors shows that six R-type MBs formed a readily discernible assembly, as indicated by the dotted circle. (**C**) Signal intensity values of all probes on chr-13, which are normalized 'per gene' to the mean expression levels in tumors 1 and 2, are indicated by colors shown at the top right.

Discussion

Radiation signatures, either genomic aberrations or gene expression profiles, that distinguish radiation-induced tumors from spontaneous tumors would be very useful for not only assessing cancer risk following low-dose radiation but also understanding the underlying mechanisms of carcinogenesis. Much effort has been made toward identifying such radiation signatures in a variety of tumors. A few studies have successfully identified genomic fingerprints of IR in human (33) and mouse (34–37) tumors. For example, LOH at *PTCH1* is more frequent in tumors from high-dose IR-exposed (≥1 Gy) atomic bomb survivors than in those from low-dose IR-exposed (<0.2 Gy) survivors (38). However, it has not yet been reported whether LOH can be practically applied for distinguishing spontaneous tumors from those induced by low-dose radiation.

Based on LOH patterns in 10 MBs, Pazzaglia *et al.* (23) suggested that distinct mechanisms are responsible for *Ptch1* loss in spontaneous versus radiation-induced MBs. Consistently, we confirmed that deletion-mediated loss of the wild-type *Ptch1* allele (R-type) can be considered a reliable radiation signature for radiation-induced MBs in *Ptch1*$^{+/-}$ mice. These data are in line with the previous reports supporting the notion that IR tends to cause interstitial deletions. The strictness in the association of deletion-mediated loss with radiation-induced MB in *Ptch1* heterozygous mice is a significant point to be emphasized. The difference in the frequency of interstitial losses between spontaneous and radiation-induced mutations was a matter of degree in the previous reports, such as those on *hprt* (hypoxanthin guanine phosphoribosyl transferase), *aprt* (adenine phosphoribosyltransferase) and *Apc* (adenomatous polyposis coli) loci (34,39,40). How interstitial loss predominates in radiation-induced tumors would depend on various factors, such as the critical gene included in the region, genetic background and allelic status of the gene (41–43). In addition, it should be mentioned that deletion-mediated loss is one of

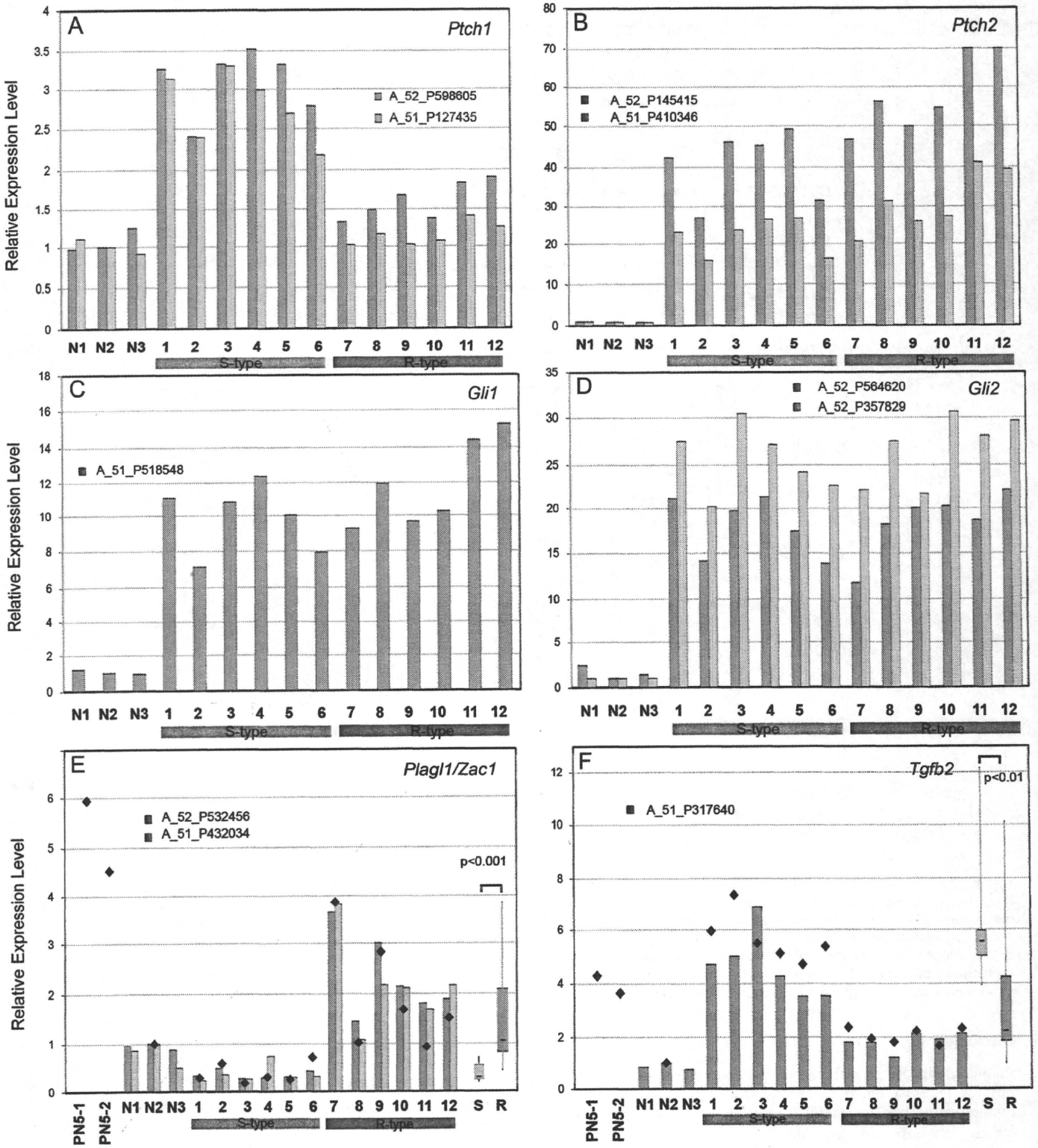

Fig. 5. Expression patterns of six genes in normal cerebellum samples and two types of MBs. Bars show the expression levels, which are relative to the expression levels in a normal cerebellum sample (N2) and are calculated based on the normalized intensity values of oligonucleotide probes in the expression microarray analysis. The name of each gene and the oligonucleotide probe is indicated in each graph. (**A–D**) Expression patterns of hedgehog target and mediator genes. (**E** and **F**) Validation of differential gene expression by quantitative reverse transcription–PCR. Expression levels after normalization to the *Gapdh* levels are indicated by filled diamonds and are relative to expression in a normal cerebellum sample (N2). In this analysis, expression levels in two normal cerebellum samples (N1 and N3) were not examined, whereas expression levels in developing cerebellum samples (PN5-1 and PN5-2) at PN5 were analyzed. Box and whisker summary plots at the right in (E) and (F) show expression levels of 12 S-type MBs (6 MBs analyzed by expression microarray analysis and additional 6 MBs) and those of 15 R-type MBs (6 MBs analyzed by expression microarray analysis and additional 9 MBs). Twelve of these additional 15 MBs (Tumor numbers are 16–30 in supplementary Table IV, available at *Carcinogenesis* Online) were selected from experimental groups with low-dose irradiation. Paired boxes represent the 25th–75th percentile expression values in S-type and R-type MBs. Horizontal bars indicate median, whereas vertical lines indicate maximum and minimum expression values.

the relevant mechanisms responsible for the inactivation of tumor suppressor genes in spontaneous tumors and that many reports have demonstrated the involvement of multiple mechanisms in inactivating tumor suppressor genes in radiation-induced tumors (44,45). In the present study, while deletion-mediated loss was perfectly associated with radiation-induced MBs from mice exposed to 3 Gy, no spontaneous-type (S-type) LOH patterns were detected in those tumors. Earlier development of R-type MBs may have prevented the appearance of S-type MBs. Alternatively, radiation may provide suppressive as well as inductive effects on spontaneous tumorigenesis. Indeed, it has been reported that early cerebellum lesions at 3 weeks of age were detected less frequently in mice exposed to 3 Gy at PN10 compared with non-irradiated control mice (46).

An important unresolved question in radiation protection is whether and how cancer risk increases dose dependently even at low doses <100 mSv or if there exists a threshold dose for radiation-induced carcinogenesis (6). Here, we have provided direct evidence of a dose-dependent increase in MBs harboring a radiation signature in *Ptch1*$^{+/-}$ mice exposed to doses at 0.05 Gy (50 mGy) to 3 Gy. The incidence of R-type tumors increased dose dependently even at low doses of 50 and 100 mGy (Figure 3), suggesting that there is no discernable threshold dose, at least for genetically susceptible mice.

Importantly, our data also suggest that the cancer risk from low-dose radiation in individuals who share one crucial genetic risk factor may vary considerably depending on genetic background. We showed that *Ptch1*$^{+/-}$ mice on the C3B6F1 background were prone to the development of radiation-induced MBs, whose susceptibility was higher than those on the CD1 background (22). In addition, Pazzaglia *et al.* have reported that *Ptch1*$^{+/-}$ mice on the C57BL/6 background are completely resistant. In connection with this resistance to radiation on the C57BL/6 background, we obtained array-CGH data showing the absence of interstitial deletions of the genomic region including *Ptch1* locus in MBs developed spontaneously (n = 3) and after 3 Gy irradiation at PN1 (n = 4) in *Ptch1*$^{+/-}$ mice on this background (data not shown), suggesting the relationship between sensitivity to radiation and the genomic radiation signature. Understanding the genetic mechanisms by which genetic backgrounds influence cancer risk will lead to better radioprotection in the future.

We found that the expression levels of hundreds of genes were closely associated with the signature and that radiation-induced MBs appeared highly similar with regard to global gene expression patterns. By integrating the data from the array-CGH analysis, we found that many of these genes reflected a signature-associated reduction in copy number on chr-13. In a recent report, human MBs were grouped into five subtypes, one of which was characterized by Shh signaling (47). Frequent deletions of the genomic region around the *PTCH1* locus were identified in this subgroup. Interestingly, gene expression levels also faithfully reflected chromosomal copy number changes in those tumors, consistent with our current results.

Many genes located on chromosomes other than chr-13 also showed differential expression patterns between tumors having or lacking the radiation signature. Differential expression of these genes might simply be indirect consequences of changes in the expression of certain genes in the deleted region on chr-13. On the other hand, differential expression may reflect other important biological aspects of radiation-induced carcinogenesis. We found an association among expression levels of genes, type of LOH (S- or R-type) and developmental stages of the cerebellum (supplementary Figure 2C is available at *Carcinogenesis* Online). Those genes included, for instances, *Plagl1/Zac1* and *Tgfb2*. *Plagl1/Zac1*, which was expressed higher in R-type MBs, is highly expressed in the external granular layer of the rat cerebellum, being maximal at PN5 through PN7 and then falling off thereafter (28). In contrast, the expression level of *Tgfb2*, which was lower in R-type MBs, is low at early PN stages in the external granular layer but considerably high at relatively later stages around PN10 (29). Together with the evidence that many other genes whose expression levels were significantly elevated in R-type tumors were also expressed maximally at early developmental stages (PN1–PN5) of the cerebellum, we hypothesized that R-type tumors had been initiated at earlier stages of cerebellar development compared with S-type tumors. This was in good agreement with that R-type tumors developed earlier than S-type ones. Earlier initiation could be one of the important causal factors for the earlier development, but another possible factor of higher proliferation rate also remains to be elucidated.

In conclusion, we present for the first time evidence that MBs in newborn *Ptch1*$^{+/-}$ mice induced by radiation, even at low doses comparable with those used for medical diagnostics, can be distinguished from spontaneous MBs not only by the interstitial deletion of the *Ptch1* locus but also by gene expression profiles partly associated with unique developmental stages.

Supplementary material

Supplementary Tables I–VI and Figures 1–3 can be found at http://carcin.oxfordjournals.org/

Funding

Grant-in-Aid from the Ministry of Education, Culture, Sports, Sciences, and Technology of Japan to Y.S. (21610029); Long-Range Research Initiative of the Japan Chemical Industry Association to S.K. (2008CC03 and 2009CC03).

Acknowledgements

The authors would like to thank Dr. Heidi Hahn and European Mouse Mutant Archive for distributing *Ptch1* heterozygous mice. The authors also thank all laboratory members for their encouragement throughout this work and the Laboratory Animal Science Section in the National Institute of Radiological Sciences for animal management.

Conflict of Interest Statement: None declared.

References

1. Berrington de Gonzalez,A. *et al.* (2009) Projected cancer risks from computed tomographic scans performed in the United States in 2007. *Arch. Intern. Med.*, **169**, 2071–2077.
2. Brenner,D.J. *et al.* (2007) Computed tomography–an increasing source of radiation exposure. *N. Engl. J. Med.*, **357**, 2277–2284.
3. Kleinerman,R.A. (2006) Cancer risks following diagnostic and therapeutic radiation exposure in children. *Pediatr. Radiol.*, **36** (suppl 2), 121–125.
4. Prasad,K.N. *et al.* (2004) Health risks of low dose ionizing radiation in humans: a review. *Exp. Biol. Med. (Maywood)*, **229**, 378–382.
5. Smith-Bindman,R. *et al.* (2009) Radiation dose associated with common computed tomography examinations and the associated lifetime attributable risk of cancer. *Arch. Intern. Med.*, **169**, 2078–2086.
6. ICRP (2007) The 2007 Recommendations of the International Commission on Radiological Protection. ICRP publication 103. *Ann. ICRP*, **37**, 1–332.
7. NRC (2005) *Health Risks from Exposure to Low Levels of Ionizing Radiation: BEIR VII-Phase 2*. The National Academies Press, Washington, DC.
8. Pierce,D.A. *et al.* (2000) Radiation-related cancer risks at low doses among atomic bomb survivors. *Radiat. Res.*, **154**, 178–186.
9. Preston,D.L. *et al.* (2003) Studies of mortality of atomic bomb survivors. Report 13: solid cancer and noncancer disease mortality: 1950–1997. *Radiat. Res.*, **160**, 381–407.
10. Cardis,E. *et al.* (2007) The 15-country collaborative study of cancer risk among radiation workers in the nuclear industry: estimates of radiation-related cancer risks. *Radiat. Res.*, **167**, 396–416.
11. Muirhead,C.R. *et al.* (2009) Mortality and cancer incidence following occupational radiation exposure: third analysis of the National Registry for Radiation Workers. *Br. J. Cancer*, **100**, 206–212.
12. Preston,D.L. *et al.* (2007) Solid cancer incidence in atomic bomb survivors: 1958–1998. *Radiat. Res.*, **168**, 1–64.
13. Mullenders,L. *et al.* (2009) Assessing cancer risks of low-dose radiation. *Nat. Rev. Cancer*, **9**, 596–604.
14. ICRP (1998) Genetic susceptibility to cancer. ICRP publication 79. Approved by the Commission in May 1997. International Commission on Radiological Protection. *Ann. ICRP*, **28**, 1–157.
15. Taipale,J. *et al.* (2001) The Hedgehog and Wnt signalling pathways in cancer. *Nature*, **411**, 349–354.

16. Marino,S. (2005) Medulloblastoma: developmental mechanisms out of control. *Trends Mol. Med.*, **11**, 17–22.
17. Romer,J. *et al.* (2005) Targeting medulloblastoma: small-molecule inhibitors of the Sonic Hedgehog pathway as potential cancer therapeutics. *Cancer Res.*, **65**, 4975–4978.
18. Gorlin,R.J. (1999) Patient described by Chun et al. may not present Antley-Bixler syndrome. *Am. J. Med. Genet.*, **83**, 64.
19. Scharnagel,I.M. *et al.* (1949) Multiple basal cell epitheliomas in a 5 year old child. *Am. J. Dis. Child.*, **77**, 647–51.
20. Goodrich,L.V. *et al.* (1997) Altered neural cell fates and medulloblastoma in mouse patched mutants. *Science*, **277**, 1109–1113.
21. Hahn,H. *et al.* (1998) Rhabdomyosarcomas and radiation hypersensitivity in a mouse model of Gorlin syndrome. *Nat. Med.*, **4**, 619–622.
22. Pazzaglia,S. *et al.* (2009) Physical, heritable and age-related factors as modifiers of radiation cancer risk in patched heterozygous mice. *Int. J. Radiat. Oncol. Biol. Phys.*, **73**, 1203–1210.
23. Pazzaglia,S. *et al.* (2006) Two-hit model for progression of medulloblastoma preneoplasia in Patched heterozygous mice. *Oncogene*, **25**, 5575–5580.
24. Yang,Z.J. *et al.* (2008) Medulloblastoma can be initiated by deletion of Patched in lineage-restricted progenitors or stem cells. *Cancer Cell*, **14**, 135–145.
25. Livak,K.J. *et al.* (2001) Analysis of relative gene expression data using real-time quantitative PCR and the 2(-Delta Delta C(T)) Method. *Methods*, **25**, 402–408.
26. Knudson,A.G. Jr. (1971) Mutation and cancer: statistical study of retinoblastoma. *Proc. Natl Acad. Sci. USA*, **68**, 820–823.
27. Knudson,A.G. (1996) Hereditary cancer: two hits revisited. *J. Cancer Res. Clin. Oncol.*, **122**, 135–140.
28. Ciani,E. *et al.* (2003) Developmental expression of the cell cycle and apoptosis controlling gene, Lot1, in the rat cerebellum and in cultures of cerebellar granule cells. *Brain Res. Dev. Brain Res.*, **142**, 193–202.
29. Constam,D.B. *et al.* (1994) Transient production of TGF-beta 2 by postnatal cerebellar neurons and its effect on neuroblast proliferation. *Eur. J. Neurosci.*, **6**, 766–778.
30. Kho,A.T. *et al.* (2004) Conserved mechanisms across development and tumorigenesis revealed by a mouse development perspective of human cancers. *Genes Dev.*, **18**, 629–640.
31. Zindy,F. *et al.* (2007) Genetic alterations in mouse medulloblastomas and generation of tumors de novo from primary cerebellar granule neuron precursors. *Cancer Res.*, **67**, 2676–2684.
32. Frappart,P.O. *et al.* (2009) Recurrent genomic alterations characterize medulloblastoma arising from DNA double-strand break repair deficiency. *Proc. Natl Acad. Sci. USA*, **106**, 1880–1885.
33. Kimmel,R.R. *et al.* (2006) Microarray comparative genomic hybridization reveals genome-wide patterns of DNA gains and losses in post-Chernobyl thyroid cancer. *Radiat. Res.*, **166**, 519–531.
34. Haines,J. *et al.* (2000) Loss of heterozygosity in spontaneous and X-ray-induced intestinal tumors arising in F1 hybrid min mice: evidence for sequential loss of APC(+) and Dpc4 in tumor development. *Genes Chromosomes Cancer*, **28**, 387–394.
35. Mao,J.H. *et al.* (2005) Genomic instability in radiation-induced mouse lymphoma from p53 heterozygous mice. *Oncogene*, **24**, 7924–7934.
36. Shimada,Y. *et al.* (2000) Radiation-associated loss of heterozygosity at the Znal (Ikaros) locus on chromosome 11 in murine thymic lymphomas. *Radiat. Res.*, **154**, 293–300.
37. Takabatake,T. *et al.* (2006) Array-CGH analyses of murine malignant lymphomas: genomic clues to understanding the effects of chronic exposure to low-dose-rate gamma rays on lymphomagenesis. *Radiat. Res.*, **166**, 61–72.
38. Mizuno,T. *et al.* (2006) Molecular basis of basal cell carcinogenesis in the atomic-bomb survivor population: p53 and PTCH gene alterations. *Carcinogenesis*, **27**, 2286–2294.
39. Park,M.S. *et al.* (1995) Molecular analysis of gamma-ray-induced mutations at the hprt locus in primary human skin fibroblasts by multiplex polymerase chain reaction. *Radiat. Res.*, **141**, 11–18.
40. Ponomareva,O.N. *et al.* (2002) Tissue-specific deletion and discontinuous loss of heterozygosity are signatures for the mutagenic effects of ionizing radiation in solid tissues. *Cancer Res.*, **62**, 1518–1523.
41. Liang,L. *et al.* (2002) Radiation-induced genetic instability *in vivo* depends on p53 status. *Mutat. Res.*, **502**, 69–80.
42. Mao,J.H. *et al.* (2003) Genetic interactions between Pten and p53 in radiation-induced lymphoma development. *Oncogene*, **22**, 8379–8385.
43. Takabatake,T. *et al.* (2008) Analysis of changes in DNA copy number in radiation-induced thymic lymphomas of susceptible C57BL/6, resistant C3H and hybrid F1 mice. *Radiat. Res.*, **169**, 426–436.
44. Kakinuma,S. *et al.* (2002) Spectrum of Znal(Ikaros) inactivation and its association with loss of heterozygosity in radiogenic T-cell lymphomas in susceptible B6C3F1 mice. *Radiat. Res.*, **157**, 331–340.
45. Yamaguchi,Y. *et al.* (2010) Complicated biallelic inactivation of Pten in radiation-induced mouse thymic lymphomas. *Mutat. Res.*, **686**, 30–38.
46. Pazzaglia,S. *et al.* (2006) Linking DNA damage to medulloblastoma tumorigenesis in patched heterozygous knockout mice. *Oncogene*, **25**, 1165–1173.
47. Kool,M. *et al.* (2008) Integrated genomics identifies five medulloblastoma subtypes with distinct genetic profiles, pathway signatures and clinicopathological features. *PLoS One*, **3**, e3088.

Received March 14, 2010; revised June 23, 2010; accepted July 3, 2010

RADIATION RESEARCH 174, 206–215 (2010)
0033-7587/10 $15.00

DOI: 10.1667/RR2006.1

DNA Copy Number Aberrations and Disruption of the p16Ink4a/Rb Pathway in Radiation-Induced and Spontaneous Rat Mammary Carcinomas

Daisuke Iizuka,[a,b] Tatsuhiko Imaoka,[a] Takashi Takabatake,[a] Mayumi Nishimura,[a] Shizuko Kakinuma,[a] Yukiko Nishimura[a] and Yoshiya Shimada[a,1]

[a] *Experimental Radiobiology for Children's Health Research Group, Research Center for Radiation Protection, National Institute of Radiological Sciences, Chiba, 263-8555, Japan; and* [b] *Department of Molecular Radiobiology, Research Institute for Radiation Biology and Medicine, Hiroshima University, Hiroshima, 734-8553, Japan*

Iizuka, D., Imaoka, T., Takabatake, T., Nishimura, M., Kakinuma, S., Nishimura, Y. and Shimada, Y. DNA Copy Number Aberrations and Disruption of the p16Ink4a/Rb Pathway in Radiation-Induced and Spontaneous Rat Mammary Carcinomas. *Radiat. Res.* 174, 206–215 (2010).

Chromosomal amplifications and deletions are thought to be important events in spontaneous and radiation-induced carcinogenesis. To clarify how ionizing radiation induces mammary carcinogenesis, we characterized genomic copy number aberrations for γ-ray-induced rat mammary carcinomas using microarray-based comparative genomic hybridization. We examined 14 carcinomas induced by γ radiation (2 Gy) and found 26 aberrations, including trisomies of chromosomes 4 and 10 for three and one carcinomas, respectively, an amplification of the chromosomal region 1q12 in two carcinomas, and deletions of the chromosomal regions 3q35q36, 5q32 and 7q11 in two, two and four carcinomas, respectively. These aberrations were not observed in seven spontaneous mammary carcinomas. The expression of *p16Ink4a* and *p19Arf*, which are located in the chromosomal region 5q32, was always up-regulated except for a carcinoma with a homozygous deletion of region 5q32. The up-regulation was not accounted for by gene mutations or promoter hypomethylation. However, the amounts of Rb and its mRNA were down-regulated in these carcinomas, indicating a disruption of the p16Ink4a/Rb pathway. This is the first report of array CGH analysis for radiation-induced mammary tumors, which reveals that they show distinct DNA copy number aberration patterns that are different from those of spontaneous tumors and those reported previously for chemically induced tumors. © 2010 by Radiation Research Society

INTRODUCTION

Ionizing radiation induces tumors in various tissues by initiating and promoting neoplastic progression (*1*). An epidemiological study of Japanese atomic bomb survivors concluded that the survivors had an higher risk of breast cancer that increased with increasing dose (*2*). The types of DNA damage induced by ionizing radiation include nucleotide/base damage, crosslinking of DNA strands, and DNA single- and double-strand breaks—all of which can lead to chromosomal abnormalities and mutations in genes. Moreover, radiation-induced genomic instability may also be an important early event in carcinogenesis (*3*).

Loss of heterozygosity, deletion of tumor suppressor genes, and amplification of proto-oncogenes are frequently observed in radiation-induced tumors (*4–6*). For the gene *Ikaros*, loss of heterozygosity is caused by genomic deletion and has been observed in radiation-induced mouse thymic lymphomas (*7*). Deletion of *Tp53* has been observed in radiation-induced mouse osteosarcomas and lymphosarcomas (*8, 9*). Conversely, *HER2* (*ERBB2*) and *C-MYC* amplifications were significantly increased in the genomes of breast cancers of Japanese atomic bomb survivors (*10*).

Genome-wide detection of DNA copy number aberrations using microarray-based comparative genomic hybridization (array CGH) is a powerful tool, and diverse aberrations have been detected in various tumors, including breast cancer (*11*). Characterization of copy number aberrations is a promising tool for discovering causative genes involved in tumorigenesis (*12*). For example, an array CGH study has revealed that rearrangement of the proto-oncogene *RET/PTC* is a radiation-specific genomic alteration in post-Chernobyl papillary thyroid carcinomas found in children (*13*). This report prompted us to investigate chromosomal abnormalities using array CGH analysis for the genomes of experimental radiation-induced mammary carcinomas.

Animal cancer models have the advantage that the causal relationship between a carcinogenic agent and structural or physiological aberrations in cancers can be studied because they are induced by a defined carcinogenic agent, in contrast to human cancers, which can

[1] Address for correspondence: Experimental Radiobiology for Children's Health Research Group, National Institute of Radiological Sciences, 4-9-1, Anagawa, Inage-ku, Chiba, 263-8555, Japan; e-mail: y_shimad@nirs.go.jp.

rarely be ascribed to a single etiological factor. Rat mammary cancer is an important experimental model for human breast cancer because these two cancers share pathological and hormonal similarities (*14*). Radiation-induced rat mammary cancer has been widely used to study radiation-associated cancer risks and the mechanisms of radiation-induced carcinogenesis (*15–19*). Prior to this report, however, no mutations or loss of heterozygosity of cancer-related genes has been observed in radiation-induced rat mammary carcinomas (*16, 18, 20*). The current study provides the first evidence that radiation-induced rat mammary carcinomas show genomic alterations including trisomy of chromosome 4, an amplification of the chromosomal region 1q12, and deletions of the chromosomal regions 3q35q36, 5q32 and 7q11, and dysregulation of the p16Ink4a/retinoblastoma (Rb) pathway.

MATERIALS AND METHODS

Animal Experiments and γ Irradiation

All animal experiments were performed in our previous study, and frozen tissue samples of mammary carcinomas were analyzed in this study [(*18*) and unpublished data]. Briefly, at 3 (n = 18) or 7 (n = 20) weeks of age, female Sprague-Dawley (Jcl:SD) rats were exposed to whole-body γ radiation (2 Gy) from a ^{137}Cs source (Gammacell; Nordion International, Ottawa, Canada) or left untreated (n = 45); rats were fed a high-corn oil (23.5%) AIN-76A diet (Clea Japan) from 9 weeks of age. Rats considered to be moribund or that survived the 1-year observation period were killed humanely by ether anesthesia, and mammary carcinomas were harvested. The multiplicities of palpable mammary carcinoma that developed before 1 year of age in untreated rats and rats irradiated at 3 or 7 weeks of age were 0.07 ± 0.04, 0.28 ± 0.11 and 0.90 ± 0.24, respectively (mean ± standard deviation) [(*18*) and unpublished data]. We randomly selected tumor samples that satisfied the following two criteria: minimum contamination by normal cells by microscopic observation and sufficient tumor size (about >1 cm in diameter) for molecular experimentation. We also performed molecular analyses of the four spontaneous mammary tumors that developed after 50 weeks of age.

Array CGH

Genomic DNA was isolated using proteinase K and phenol-chloroform extraction. Array CGH used the reagents of Rat Genome CGH Microarray 105A kits (Agilent Technologies, Palo Alto, CA) and the version 4 protocol. In brief, genomic DNA from either ear skin or normal mammary tissue of each rat was used as the reference hybridization. One microgram each of digested tumor DNA and reference DNA was labeled with Cy5- or Cy3-dUTP, respectively (Agilent Technologies). After hybridization of labeled DNA with the microarray DNAs, fluorescence intensity data were obtained using a DNA microarray scanner (DNA Microarray Scanner, Model G2565BA; Agilent Technologies) and expressed numerically using the Agilent Feature Extraction software (version 9.5.1) and the manufacturer's recommended settings. The CGH Analytics software (version 3.5.14; Agilent Technologies) was used for statistical analyses. All regions of statistically significant copy number changes were determined using the Aberration Detection Method-2 (ADM-2) algorithm with a threshold of 4.1 and were displayed as the mean of the $\log_2$ ratio for each region. The microarray data reported herein have been deposited in the Gene Expression Omnibus database (www.ncbi.nlm.nih.gov/geo; accession no. GSE16128).

TABLE 1
Primer Pairs for PCR

Gene symbol	Forward primer Reverse primer[a]
Sodium bisulfite DNA sequencing	
p16Ink4a	TTTTAAGGGGTGGTTAGGTTTG
	AAAATTATCTCACTACAAATAAAACATTCC
Reverse transcription (RT)-PCR analysis	
p15Ink4b	CGAGGCTGTAACAATCTCAAGG
	CCTAGATAGGGCTGGGGAGAA
p16Ink4a	GAAGGCGAACTCGAGGAGAG
	CAGAAGTGAAGCCAAGGAGAAAA
p19Arf	AGCATGGGTCGCAGGTT
	CCAGAAGTGAAGCCAAGGAG
rGapdh	GGTGAAGGTCGGTGTGAACG
	GGGTTTCCCGTTGATGACCA
Quantitative RT-PCR	
p15Ink4b	AGATCCCAACGCCGTCAA
	ATCATGCACAGGTCTGGTGAG
p16Ink4a	CCTAGAGCGGGGACATCACG
	TAGCGCTGCTTTGGGGGTTG
p19Arf	GGTGTTGAGGCCAGAGAGGA
	GCACCATAGGAGAGCAGGAGAG
Rb	ACGAAAAAGCAACCCTGATG
	TCTGATGGCTGATCACTTGC

[a] Base sequences are indicated in the order of 5′ to 3′.

Sodium Bisulfite DNA Sequencing

The methylation status of the *p16Ink4a* promoter region was determined by sequencing it after treating genomic DNA with the reagents of a CpGenome DNA Modification kit (Chemicon International, Temecula, CA) according to the manufacturer's instructions. The bisulfite-modified DNA was PCR-amplified using the primers listed in Table 1. The PCR products were cloned into pCR2.1-TOPO vectors using the reagents of a TA cloning kit (TOPO TA Cloning® kit, Invitrogen, Carlsbad, CA) according to the manufacturer's instructions. To determine the CpG methylation status of the promoter region, more than five clones per mammary carcinoma were sequenced using the reagents of an ABI PRISM Dye Deoxy Terminator Cycle Sequencing kit and an ABI 3100 DNA Sequencer (Applied Biosystems, Foster City, CA).

Reverse Transcription (RT)-PCR Analysis

Total RNA was extracted from frozen tumor samples using a standard acid guanidinium phenol chloroform method (Isogen; Nippon Gene Co., Tokyo, Japan) and purified using silica-gel membranes (RNeasy Mini kit; Qiagen Inc., Valencia, CA). First-strand cDNA was synthesized using 5 μg of total RNA, random primers and a modified, recombinant reverse transcriptase (ReverTra Ace, Toyobo, Osaka, Japan) in a 20-μl reaction volume. All amplifications were performed using 5 μl of a 1:50-diluted cDNA sample, 0.4 U AccuPrime™ Taq High Fidelity (Invitrogen), 1× AccuPrime™ PCR Buffer I, and 0.2 μ*M* sense and antisense primers. Cycling conditions were: for *Gapdh* (glyceraldehyde-3-phosphate dehydrogenase), initial denaturation at 94°C for 2 min, followed by 27 cycles at 94°C for 30 s, 60°C for 30 s and 68°C for 60 s, and for *p15Ink4b*, *p16Ink4a* and *p19Arf*, initial denaturation at 94°C for 2 min, followed by 35 cycles at 94°C for 30 s, 60°C for 30 s and 68°C for 60 s. The primer sequences are listed in Table 1. PCR-amplified products were electrophoresed through 2% agarose gels, stained with ethidium bromide, and, after extraction, sequenced as described above.

TABLE 2
DNA Copy Number Aberrations of Rat Mammary Carcinoma in an Array-CGH Analysis

A) Mammary carcinomas induced by irradiation at 3 weeks of age

	Locus		Log_2 ratio		
Tumor ID	Chromosome	Length (Mb)	Gain	Loss	Number of genes involved[c]
M1493-1	4q11q44	186.6	0.16[a]		549 genes
	5q32	0.4		−2.43	3 genes
	7q11	5.9		−0.18	—
M1180-1	7q11	3.4		−0.11	—
M1496-4	10q11q32.3	110.7	0.13[b]		641 genes
M1499-2	1q42	0.7	0.31		6 genes
	3q42	0.5	0.25		2 genes
M1501-4	ND				
M1495-1	1q12	2.6	0.28		—
	4q11q44	187.0	0.33[a]		549 genes
	4q42	0.2		−0.04	1 gene
	Xq13	1.3		−0.15	5 genes
M1501-2	5q32	0.4		−0.81	3 genes

B) Mammary carcinomas induced by irradiation at 7 weeks of age

	Locus		Log_2 ratio		
Tumor ID	Chromosome	Length (Mb)	Gain	Loss	Number of genes involved
M1192-1	2q26q34	38.7		−0.2	74 genes
	3q21	0.2		−0.33	—
M1197-2	3q35q36	1.6		−0.66	6 genes
M1222-4	18q12.3	0.4		−0.31	—
M1182-1	4q11q44	186.9	0.1[a]		549 genes
	4q42	1.6		−0.09	7 genes
	7q11	6.0		−0.09	—
	Xq21q22	26.6		−0.19	50 genes
M1113-3	ND				
M1148-4	3q34q36	17.4		−0.14	69 genes
M1113-2[d]	1q12	2.6	0.26		—
	4q31	0.3		−0.47	1 gene
	6q24	0.3		−0.28	—
	7q11	5.7		−0.19	—
	10q24	0.3		−0.19	—

C) Spontaneous mammary carcinomas

	Locus		Log_2 ratio		
Tumor ID	Chromosome	Length (Mb)	Gain	Loss	Number of genes involved
M1298-1	10q31	0.2	0.31		4 genes
M1299-2	ND				
M1622-1	ND				
M1212-1	ND				
M1592-2	ND				
M1699-1	ND				
M1643-2	2q44q45	12.2	0.14		30 genes

D) Comparison between etiologies

	Etiology		
Item	Radiation	Spontaneous	*P* value
Any aberration	12/14 (86%)	2/7 (29%)	<0.05*
Any deletion	10/14 (71%)	0/7 (0%)	<0.005*
Any amplification	6/14 (43%)	2/7 (29%)	>0.05*
Number of aberrations	1.9 ± 0.4	0.3 ± 0.2	<0.01†
Number of deletions	1.3 ± 0.3	0.0 ± 0.0	<0.005†
Number of amplifications	0.6 ± 0.2	0.3 ± 0.2	>0.05†

Continued